Engineering Optimization, Volume 46, Issue 3, 2014

Robust Design with Imprecise Random Variables and Its application in Hydrokinetic Turbine Optimization

Zhen Hu and Xiaoping Du[1]
Department of Mechanical and Aerospace Engineering
Missouri University of Science and Technology
Rolla, MO 65409, U.S.A.

Nitin S. Kolekar and Arindam Banerjee
Department of Mechanical Engineering and Mechanics
Lehigh University
Bethlehem, PA 18015, U.S.A.

[1] Corresponding author, 400 West 13th Street, Toomey Hall 290D,Rolla, MO 65401, U.S.A., Tel: 1-573-341-7249, e-mail: dux@mst.edu

Abstract

In robust design, uncertainty is commonly modeled with precise probability distributions. In reality, the distribution types and distribution parameters may not always be available due to limited data. This research develops a robust design methodology to accommodate the mixture of both precise and imprecise random variables. By incorporating the Taguchi quality loss function and the minimax regret criterion, the methodology mitigates the effects of not only uncertain parameters but also uncertainties in the models of the uncertain parameters. Hydrokinetic turbine systems are a relatively new alternative energy technology, and both precise and imprecise random variables exist in the design of such systems. The developed methodology is applied to the robust design optimization of a hydrokinetic turbine system. The results demonstrate the effectiveness of the proposed methodology.

Keywords: robust design, uncertainty, optimization, hydrokinetic energy

1. Introduction

Robust design (Taguchi 1993, Taguchi *et al.* 2000) is a design methodology that determines optimal design variables so that the effects of noises (uncertainties) are minimized. If robustness is achieved, the performances of a product will not be sensitive to variations within the product or in its operating environment. As a result, a robust product can perform its intended function properly in the presence of uncertainties.

The key to robust design is the management of uncertainty. Uncertainty exists in any engineering systems. Uncertainty may come from stochastic physical nature; for example, the ultimate stress of composite materials, the temperature of an engine, and the river flow velocity of a hydrokinetic turbine, are all random. Uncertainty may also come from the lack of knowledge or scarcity of data. The ignorance and mistreatment of uncertainty may lead to quality losses (Dubey and Yadava 2008) or even catastrophe (Radaev 2000). As a major approach to uncertainty initiated by Taguchi (Taguchi 1993, Taguchi *et al.* 2000), robust design has been widely investigated and applied (Youn *et al.* 2007, Choi *et al.* 2008, Lu and Li 2009, Lu *et al.* 2010, Ruderman *et al.* 2010, Saha and Ray 2011). For instance, Ramakrishnan (Ramakrishnan and Rao 1996) proposed a quality loss function for the robust design of general design situations. Karpel (Karpel *et al.* 2003) applied the robust design method to the optimization of aeroservoelastic design. Du (Du and Chen 2000, Du and Chen 2002) developed an efficient robust design method for multidisciplinary design optimization problems, which are subjected to uncertain parameters and uncertain models. By using the computationally expensive finite element simulations, Wiebenga (Wiebenga *et al.* 2012) developed a generally applicable strategy for modeling and efficiently solving robust optimization problems. Similarly, Papadimitriou (Papadimitriou and Giannakoglou 2012) applied the third-order sensitivity derivatives for robust aerodynamic design to account for environmental uncertainties.

In the above robust design methods, uncertain variables are usually treated as random variables, whose distributions are assumed precisely known. This kind of uncertainty is usually referred to as aleatory uncertainty (Dolšek 2012, Du 2012). Aleatory uncertainty is also called objective uncertainty, which arises from natural variability and is irreducible. Representative examples include variations in material properties and variation of product dimensions due to manufacturing imprecision. In many engineering applications, however, precise probability distributions may not always be available due to the lack of sufficient data (Utkin 2004). As a result, there is also uncertainty in the models of the above mentioned aleatory uncertainties. This additional or secondary uncertainty is called epistemic uncertainty (Baillie *et al.* 2008, Du 2008, Huang and Zhang 2009, Veneziano *et al.* 2009). For instance, the river velocity of the hydrokinetic turbine is associate with aleatory uncertainty because the natural variability is inherent in the river flow climate (Hu and Du 2012). But most of the time, the recorded historical river velocity data are too limited to precisely describe the river velocity with a specified probabilistic model. Instead, several

hypothetical probabilistic models may be applicable for modeling the river velocity. In this situation, the model of the river velocity is also associated with epistemic uncertainty in the design of a hydrokinetic turbine system. The widely used approaches to epistemic uncertainty or imprecise random variables include (1) interval arithmetic, (2) fuzzy sets, (3) imprecise probability theory, and (4) modeling the imprecise random variables with several candidate distributions. However, in most traditional robust design methodologies, only the precise probability theory is employed.

In the past decades, many progresses were made in the related areas. For instance, for uncertainty analysis with imprecise random variables, Han and Jiang proposed a hybrid reliability analysis approach for problems with limited information (Jiang *et al.* 2012). Du (Du 2008) developed a unified uncertainty analysis method based on the evidence theory. In the area of reliability-based design (RBD) with imprecise random variables (Walley 1991, Weichselberger 2000), Aughenbaugh (Aughenbaugh and Paredis 2006) discussed the significance of using imprecise probabilities in engineering design. Based on the imprecise probability theory, Utkin (Ahmad and Kamaruddin 2012) developed a method for estimating the bounds for the structural reliability. Nikolaidis and Mourelatos (Nikolaidis and Mourelatos 2011) applied the polynomial chaos expansion (PCE) method to the approximation of reliability upper and lower bounds for systems with imprecise random variables. Herrmann (Herrmann 2009) presented an approach for solving imprecise probability design optimization problems.

The imprecise probability for RBD could be extended to robust design. When the imprecise probability is applied to the robust design, however, it is difficult for decision makers to determine which probability level or hypothetical model should be employed for the optimization even if probability bounds can be provided by the P-box (Aughenbaugh and Paredis 2006). Moreover, no matter which bound or model is used for optimization, it always brings regrets to the decision maker. The reason is that another bound or model may be better than the one used (Li and Huang 2006, Conde and Candia 2007). It is therefore worthwhile to quantify the regret and ultimately minimize it during the robust optimization process. Using the minimax-regret (MMR) criterion (Zhang 2011, Stoye 2012) can be a solution to the aforementioned problem.

The MMR criterion has been widely applied in policy management, optimization, and decision making under uncertainty (Renou and Schlag 2010, Renou and Schlag 2011, Stoye 2011). It is known as an effective method to identify the strategy, which minimizes the maximum regret or loss when the information of system variables is insufficient. For example, a method was proposed for a linear programming problem with interval objective function using the MMR criterion (Inuiguchi and Kume 1991, Inuiguchi and Sakawa 1995). After incorporating the MMR analysis framework into the interval-parameter programming, Li and Huang (Li and Huang 2009, Li *et al.* 2009) developed an interval MMR programming method. Chang and Davila (Chang

and Davila 2007) applied the MRR analysis method to address uncertainties in waste streams in major cities and improve solid waste management strategies. From the literature reviews it can be found that most of the applications of the MMR decision criterion are limited to the policy management. The purpose of this work is to integrate the MMR criterion and robust design so that the optimal design variables can be determined with both precise and imprecise random variables in engineering applications. The Taguchi quality loss function is employed to evaluate the robustness of product performance, and the MMR criterion is used to minimize the effect of uncertainty or maximize the robustness.

As a new technology for alternative energy, hydrokinetic turbines have attracted much attention recently. During the development of a new hydrokinetic turbine system (Hu *et al.* 2012), many challenges exist, including the treatment of imprecise random river flow velocity. The proposed method was then applied to the robust design optimization of the hydrokinetic turbine system. Promising results have been obtained.

The remainder of this paper is organized as follows. Section 2 reviews the traditional robust design methodology for random variables with precise probability distributions. Section 3 discusses the types of imprecise random variables. The effects of random variables are then investigated in Section 4. Section 5 presents the robust design method with precise and imprecise random variables. The developed method is then applied to the design optimization of a hydrokinetic turbine in Section 6. Conclusions are drawn in Section 7.

2. Robust design with aleatory uncertainty

In this section, the traditional robust design method is reviewed. The method is based on the Taguchi quality loss function (QLF) for problems with precisely known random variables.

2.1 Taguchi quality loss function (QLF)

The Taguchi QLF is widely used as a robustness metric in robust design optimization (Chen *et al.* 1999). There are three types of performance variables, which are referred to as quality characteristics (QCs), in a QLF. They are nominal-the-best QCs, smaller-the-better QCs, and larger-the-better QCs. The QLF can explicitly represent the effect of a deviation from the target on the quality loss. Minimizing the expected quality loss can bring the mean value of a nominal-the-best QC to its target and reduce the variability of the QC simultaneously.

Define Z as a QC. The QLF of a nominal-the-best QC is given by (Tsui 1992)

$$L(Z,T) = k(Z-T)^2 \tag{1}$$

where k is the quality loss coefficient, and T is the target or desired value of Z.

The QLFs for a smaller-the-better and a larger-the-better QC are given by

$$L(Z) = kZ^2 \tag{2}$$

and

$$L(Z) = k / Z^2 \tag{3}$$

respectively.

In this work, the nominal-the-best QC is employed. The expected quality loss is

$$C(\mu_Z, \sigma_Z) = E[L(Z, T)] = k[\sigma_Z^2 + (\mu_Z - T)^2] \tag{4}$$

and μ_Z and σ_Z are the mean and standard deviation of *Z*, respectively.

2.2 Robust design based on the Taguchi quality loss function

Let Z be given by

$$Z = f(\mathbf{d}, \mathbf{X}) \tag{5}$$

where $\mathbf{d} = (d_1, d_2, \cdots, d_n)$ is the vector of design variables, $f(\cdot)$ is the response function, and $\mathbf{X} = (X_1, X_2, \cdots, X_m)$ is a vector of random variables whose distributions are precisely known.

With the Taguchi QLF, a robust design model for problems with precisely known random variables is given as follows:

$$\begin{cases} \min\limits_{\mathbf{d}} C(\mu_Z(\mathbf{d}, \mathbf{X}), \sigma_Z(\mathbf{d}, \mathbf{X})) \\ \text{subject to} \\ g_i(\mathbf{d}, \boldsymbol{\mu}_\mathbf{X}) \le 0, i = 1, 2, \cdots, n_i \\ h_j(\mathbf{d}, \boldsymbol{\mu}_\mathbf{X}) = 0, \ j = 1, 2, \cdots, n_e \\ \Pr\{m_k(\mathbf{d}, \mathbf{X}) < 0\} \ge P_k, k = 1, 2, \cdots, n_u \\ \mathbf{d}^L \le \mathbf{d} \le \mathbf{d}^U \end{cases} \tag{6}$$

where

— $\boldsymbol{\mu}_\mathbf{X}$ are the mean values of $\mathbf{X}$;

— $g_i(\mathbf{d}, \boldsymbol{\mu}_\mathbf{X}) \le 0, i = 1, 2, \cdots, n_i$ are deterministic inequality constraint functions;

— $h_j(\mathbf{d}, \boldsymbol{\mu}_\mathbf{X}) = 0, \ j = 1, 2, \cdots, n_e$ are deterministic equality constraint functions;

— $\Pr\{m_k(\mathbf{d}, \mathbf{X}) < 0\} \ge P_k, k = 1, 2, \cdots, n_u$ are the probabilistic constraint functions;

— $\mathbf{d}^L$ and $\mathbf{d}^U$ are lower and upper bounds of $\mathbf{d}$, respectively;

— $\mu_Z(\mathbf{d}, \mathbf{X})$ and $\sigma_Z(\mathbf{d}, \mathbf{X})$ are the mean and standard deviation of Z, respectively.

$\mu_Z(\mathbf{d}, \mathbf{X})$ and $\sigma_Z(\mathbf{d}, \mathbf{X})$ can be calculated either by analytical methods or by Monte Carlo simulation (MCS).

With analytical methods,

$$\mu_Z(\mathbf{d}, \mathbf{X}) = \int_{-\infty}^{\infty} f(\mathbf{d}, \mathbf{X}) p_\mathbf{X}(\mathbf{X}) d\mathbf{X} \tag{7}$$

$$\sigma_Z(\mathbf{d}, \mathbf{X}) = \sqrt{\int_{-\infty}^{\infty} [f(\mathbf{d}, \mathbf{X}) - \mu_f(\mathbf{d}, \mathbf{X})]^2 p_\mathbf{X}(\mathbf{X}) d\mathbf{X}} \tag{8}$$

where $p_\mathbf{X}(\mathbf{X})$ is the joint probability density function (PDF) of $\mathbf{X}$.

With MCS,

$$\mu_Z(\mathbf{d}, \mathbf{X}) = \frac{1}{N}\sum_{i=1}^{N} f(\mathbf{d}, \mathbf{x}_i) \tag{9}$$

$$\sigma_Z(\mathbf{d}, \mathbf{X}) \cong \sqrt{\frac{1}{N-1}\sum_{i=1}^{N}[f(\mathbf{d}, \mathbf{x}_i) - \mu_Z(\mathbf{d}, \mathbf{X})]^2} \tag{10}$$

where N is the number of samples, and $\mathbf{x}_i$ is the *i*-th sample of $\mathbf{X}$.

MCS generally requires hundreds of calls of function $Z = f(\mathbf{d}, \mathbf{X})$. If the function is computationally cheap, MCS can be employed. Otherwise, an analytical method should be used. However, when the dimension of $\mathbf{X}$ is large, Eqs. (9) and (10) for the analytical method may also be computationally expensive because of the high-dimensional integrals. In this case, other approximation methods may be used (Madsen 1986, Du *et al.* 2005, Huang and Du 2008, Zhang and Du 2010, Banerjee and Smith 2011, Kim *et al.* 2011, Millwater and Feng 2011).

3. Imprecise random variables

Probability distributions are usually obtained from statistical data. When the data are limited, obtaining a precise distribution is difficult, and the following types of imprecise random variables may be encountered:

- Type I – Random variables with multiple candidate distributions
- Type II – Probability distributions whose parameters, such as means and standard deviations, are also uncertain

In this paper, an imprecise random variable is denoted by $\tilde{Y}$.

3.1 Random variables with multiple candidate distributions

When statistical data are not sufficient to produce a precise distribution, several candidate distributions, which can fit the data well, may be obtained. Without any prior knowledge about the distribution of a random variable, a standard procedure of hypothesis testing (McGill *et al.* 2006) can be followed by making a hypothesis that the random variable follows distribution A. The hypothesis test can be performed for distributions B, C, D, and so on. If the sample size of the data is not large enough, it is common that several distributions, such as distributions A, B, C, and D, can pass the hypothesis test. When this happens, multiple candidate distributions can be used to describe a single random variable, and the distribution is therefore not precisely known. Fig. 1 shows the cumulative probability density function (CDF) of an imprecise random variable with three possible distributions.

Place Fig. 1 here

This situation is commonly encountered in practical applications. For example, the wind speed of a wind turbine at different locations may be described by a Weibull, Generalized Rayleigh, Lognormal, or Kappa distribution (He 2009, Morgan *et al.*

2011). The initial crack size of materials is suggested to be a Lognormal or Weibull distribution (Zhang and Mahadevan 2000). Similarly, the equivalent initial flaw size may be modeled as a Lognormal, Weibull, or three-parameter Weibull distribution (Maymon 2005, Cross *et al.* 2007, Makeev *et al.* 2007). When data are too limited, all these empirical models can be used as candidate distributions for the imprecise random variable.

3.2 Random variables with imprecise distribution parameters

For this case, the distribution type of a random variable may be known, but the distribution parameters may not be precise. A distribution parameter such as the mean is typically estimated from data available. The confidence of the estimation largely depends on the sample size. The larger is the sample size, the higher is the confidence. The estimate may be given within an interval, which is usually called the confidence interval. At a certain confidence level, the width of the confidence interval depends on the sample size. When the sample size is large, the width of the confidence interval is small, and the midpoint of the interval can then be used as the associated distribution parameter. If the sample size is too small, however, the interval will be wide. In this case, the midpoint cannot be simply used, and then the random variable has imprecise distribution parameters.

Let $\tilde{Y}$ be a random variable with imprecise distribution parameters and $p_{\tilde{Y}} = f_p(y, \tilde{\mathbf{r}}_Y)$ be its probability density function (PDF). Suppose the distribution parameters are

$$\tilde{\mathbf{r}}_Y \in [\underline{\mathbf{r}}_Y, \overline{\mathbf{r}}_Y] \tag{11}$$

in which $\tilde{\mathbf{r}}_Y$ is the vector of distribution parameters, and $\underline{\mathbf{r}}_Y$ and $\overline{\mathbf{r}}_Y$ are the lower and upper bounds, respectively.

As an example, Fig. 2 shows the CDF curves of an imprecise random variable $\tilde{Y}$ with a known normal distribution, known standard deviation, but an imprecise mean. Figs. 3 and 4 present the CDF curves of a normal random variable with an imprecise standard deviation and with both imprecise mean and standard deviation, respectively.

Place Figs. 2-4 here

To account for the random variables with imprecise distribution parameters, the p-box method (Aughenbaugh and Paredis 2006) can be used, where a p-box expresses the CDF of imprecise random variable by interval bounds as indicated in Figs. 2 through 4. However, no matter which bounds are used, they may always result in regrets. A new method is needed to accommodate imprecise random variables for

robust design. In the next section, the effects of imprecise random variables on the robustness of a product are further explained, and a new robust design method is then developed using the MMR criterion to minimize the regrets due to the impreciseness.

4. General effects of random variables

Robust design optimization is used to minimize the effects of uncertainties during the design process. The effects of both aleatory and epistemic uncertainties are explained below.

4.1. Effects of aleatory uncertainty (precise random variables)

Due to the involvement of aleatory uncertainty, the performance variable Z is also a random variable. To make the performance insensitive to aleatory uncertainty, robust design optimization presented in Sec. 2 brings the mean of Z to its target and at the same time reduces the standard deviation of Z. Fig. 5 illustrates the PDF of Z before and after robust design optimization. After the optimization, the distribution of Z is shifted to the target, and the distribution is also shrunk.

Place Fig. 5 here

4.2. Effects of epistemic uncertainties

When there are also imprecise random variables $\tilde{\mathbf{Y}}$, the performance function given in Eq. (5) becomes

$$Z = f(\mathbf{d}, \mathbf{X}, \tilde{\mathbf{Y}}) \tag{12}$$

As discussed in Sec.3, there may be several models for the distribution of an imprecise random variable. If only one of them is used in the robust design optimization described in Sec. 2, the obtained solution may not be optimal for other models.

In fact, the performance variable Z is a random variable because it is a function of random variables $\mathbf{X}$, and it is also an imprecise random variable because it is also a function of imprecise random variables $\tilde{\mathbf{Y}}$. As a result, the mean and standard deviation of Z will not be singled-valued quantities. The task of this work is to develop a new robust design optimization approach to deal with the combined aleatory and epistemic uncertainty.

5. Robust design with the mixture of aleatory and epistemic uncertainties

The new robust design optimization method is built upon the Taguchi QLF and the

MMR criterion, which will be reviewed first. Then the new robust design optimization method is discussed.

5.1 The MMR criterion

The MMR criterion has been adopted for decision making when the information of input variables are incomplete (Manski 2007, Tetenov 2012). Let $\mathbf{U} = [\mathbf{u}^{(1)}, \mathbf{u}^{(2)}, \cdots, \mathbf{u}^{(n)}]$ be a vector of the candidate models for the imprecise random variables $\tilde{\mathbf{U}}$ and $\mathbf{s}_i^*$ be the optimal strategy for the design obtained from the assumption that only the *i*-th model $\mathbf{u}^{(i)}$ is correct.

The regret of strategy $\mathbf{s}$ with respect to *i*-th model $\mathbf{u}^{(i)}$ is given by

$$R(\mathbf{s}, \mathbf{u}^{(i)}) = V(\mathbf{s}, \mathbf{u}^{(i)}) - V(\mathbf{s}_i^*, \mathbf{u}^{(i)}) \tag{13}$$

where $V(\mathbf{s}, \mathbf{u}^{(i)})$ is the quality loss of strategy $\mathbf{s}$ if the QLF is used. Eq. (13) indicates that $R(\mathbf{s}, \mathbf{u}^{(i)})$ is always positive.

The maximum regret of strategy $\mathbf{s}$ is then computed by

$$R_{\max}(\mathbf{s}, \mathbf{U}) = \max\{R(\mathbf{s}, \mathbf{u}^{(j)}),\ j = 1, 2, \cdots, n\} \tag{14}$$

According to the MMR criterion, the optimal strategy for the vector of imprecise information $\mathbf{U}$ is defined as

$$\mathbf{s}^* = \arg\min_{\mathbf{d}} R_{\max}(\mathbf{s}, \mathbf{U}) \tag{15}$$

The minimax analysis is formulated as an optimization problem as follows:

$$\begin{cases} MMR = \underset{\mathbf{s}}{\text{Min}} \left\{ \underset{\mathbf{u}}{\text{Max}}[R(\mathbf{s}, \mathbf{u}^{(i)})] \right\} \\ \text{subject to} \\ g_i(\mathbf{s}) \le 0,\ i = 1, 2, \cdots, n_i \\ h_j(\mathbf{s}) = 0,\ j = 1, 2, \cdots, n_e \end{cases} \tag{16}$$

where $\mathbf{s} = [s_1, s_2, \cdots, s_n]$ is the space of strategies.

5.2 Robust design based on the MMR criterion

As discussed in Sec. 5.1, the MMR criterion can minimize the regret for decision making under uncertainty. In this section, robust design methods with precise and imprecise random variables are introduced based on the MMR criterion. For different types of imprecise random variables, three models are proposed.

5.2.1. Model 1 — Robust design with Type I imprecise random variables

Let $\tilde{\mathbf{Y}}$ be the vector of imprecise random variables. For Type I imprecise random variables, $\tilde{\mathbf{Y}}$ is given by

$$\tilde{\mathbf{Y}} = [\mathbf{Y}^{(1)}, \mathbf{Y}^{(2)}, \cdots, \mathbf{Y}^{(n)}] \tag{17}$$

where $\mathbf{Y}^{(i)}$ stands for the *i*-th hypothetical distributions for $\tilde{\mathbf{Y}}$.

With the MMR criterion, the following robust design optimization model is

proposed:

$$\begin{cases} \min\limits_{\mathbf{d}} R_{\max}(\mathbf{d}) \\ \text{subject to} \\ R_{\max}(\mathbf{d}) = \max\{r(\mathbf{d}, \mathbf{X}, \mathbf{Y}^{(1)}), r(\mathbf{d}, \mathbf{X}, \mathbf{Y}^{(2)}), \cdots, r(\mathbf{d}, \mathbf{X}, \mathbf{Y}^{(n_h)})\} \\ r(\mathbf{d}, \mathbf{X}, \mathbf{Y}^{(i)}) = C(\mu_Z(\mathbf{d}, \mathbf{X}, \mathbf{Y}^{(i)}), \sigma_Z(\mathbf{d}, \mathbf{X}, \mathbf{Y}^{(i)})) \\ \qquad\qquad - C(\mu_Z(\mathbf{d}_{opt}^{(i)}, \mathbf{X}, \mathbf{Y}^{(i)}), \sigma_Z(\mathbf{d}_{opt}^{(i)}, \mathbf{X}, \mathbf{Y}^{(i)})), i = 1, 2, \cdots n_h \\ g_j(\mathbf{d}, \boldsymbol{\mu}_{\mathbf{X}}, \boldsymbol{\mu}_{\mathbf{Y}^{(i)}}) \le 0,\ j = 1, 2, \cdots, n_j;\ i = 1, 2, \cdots n_h \\ h_k(\mathbf{d}, \boldsymbol{\mu}_{\mathbf{X}}, \boldsymbol{\mu}_{\mathbf{Y}^{(i)}}) = 0,\ k = 1, 2, \cdots, n_e;\ i = 1, 2, \cdots n_h \\ \Pr\{m_l(\mathbf{d}, \mathbf{X}, \mathbf{Y}^{(i)}) < 0\} \ge P_l,\ l = 1, 2, \cdots, n_u;\ i = 1, 2, \cdots n_h \\ \mathbf{d}^L \le \mathbf{d} \le \mathbf{d}^U \end{cases} \tag{18}$$

where n_h is the number of hypothetical distributions, $r(\mathbf{d}, \mathbf{X}, \mathbf{Y}^{(i)})$ is the regret of the design obtained from the *i*-th hypothetical distribution, $R_{\max}(\mathbf{d})$ is the maximum regret, and $\mathbf{d}_{opt}^{(i)}, i = 1, 2, \cdots n_h$ is the optimal design by using the *i*-th hypothetical distribution from the following optimization model:

$$\begin{cases} \min\limits_{\mathbf{d}} C(\mu_Z(\mathbf{d}_{opt}^{(i)}, \mathbf{X}, \mathbf{Y}^{(i)}), \sigma_Z(\mathbf{d}_{opt}^{(i)}, \mathbf{X}, \mathbf{Y}^{(i)})) \\ \text{subject to} \\ g_j(\mathbf{d}_{opt}^{(i)}, \boldsymbol{\mu}_{\mathbf{X}}, \boldsymbol{\mu}_{\mathbf{Y}^{(i)}}) \le 0,\ j = 1, 2, \cdots, n_j \\ h_k(\mathbf{d}_{opt}^{(i)}, \boldsymbol{\mu}_{\mathbf{X}}, \boldsymbol{\mu}_{\mathbf{Y}^{(i)}}) = 0,\ k = 1, 2, \cdots, n_e \\ \Pr\{m_l(\mathbf{d}, \mathbf{X}, \mathbf{Y}^{(i)}) < 0\} \ge P_l,\ l = 1, 2, \cdots, n_u \\ \mathbf{d}^L \le \mathbf{d}_{opt}^{(i)} \le \mathbf{d}^U \end{cases} \tag{19}$$

$\mu_Z(\mathbf{d}_{opt}^{(i)}, \mathbf{X}, \mathbf{Y}^{(i)})$ and $\sigma_Z(\mathbf{d}_{opt}^{(i)}, \mathbf{X}, \mathbf{Y}^{(i)})$ are solved using Eqs. (7) and (8) or (9) and (10).

5.2.2. Model 2 — Robust design with Type II imprecise random variables

Let $\tilde{\mathbf{Y}}$ be the vector of imprecise random variables. For Type II imprecise random variables, $\tilde{\mathbf{Y}}$ is presented by

$$\tilde{\mathbf{Y}} = \mathbf{Y}(\tilde{\mathbf{r}}_Y), \tilde{\mathbf{r}}_Y \in [\underline{\mathbf{r}}_Y, \overline{\mathbf{r}}_Y] \tag{20}$$

in which $\mathbf{Y}(\tilde{\mathbf{r}}_Y)$ are the vectors of random variables $\tilde{\mathbf{Y}}$ given the imprecise distribution parameters $\tilde{\mathbf{r}}_Y$.

Then the robust design optimization model is given by

$$
\begin{cases}
\min\limits_{\mathbf{d}} R_{\max}(\mathbf{d}) \\
\text{Subject to} \\
R_{\max}(\mathbf{d}) = \max\limits_{\tilde{\mathbf{r}}_Y} r(\mathbf{d}, \tilde{\mathbf{r}}_Y) \\
\quad \begin{cases}
\text{Subject to} \\
r(\mathbf{d}, \tilde{\mathbf{r}}_Y) = C(\mu_Z(\mathbf{d}, \mathbf{X}, \mathbf{Y}(\tilde{\mathbf{r}}_Y)), \sigma_Z(\mathbf{d}, \mathbf{X}, \mathbf{Y}(\tilde{\mathbf{r}}_Y))) \\
-C(\mu_Z(\mathbf{d}_{opt}, \mathbf{X}, \mathbf{Y}(\tilde{\mathbf{r}}_Y)), \sigma_Z(\mathbf{d}_{opt}, \mathbf{X}, \mathbf{Y}(\tilde{\mathbf{r}}_Y))) \\
\quad \begin{cases}
\mathbf{d}_{opt} = \\
\min\limits_{\mathbf{d}_t} C(\mu_Z(\mathbf{d}_t, \mathbf{X}, \mathbf{Y}(\tilde{\mathbf{r}}_Y)), \sigma_Z(\mathbf{d}_t, \mathbf{X}, \mathbf{Y}(\tilde{\mathbf{r}}_Y))) \\
\text{Subject to} \\
\begin{cases}
g_j(\mathbf{d}_t, \boldsymbol{\mu}_{\mathbf{X}}, \boldsymbol{\mu}_{\mathbf{Y}(\tilde{\mathbf{r}}_Y)}) \le 0,\ j = 1, 2, \cdots, n_j \\
h_k(\mathbf{d}_t, \boldsymbol{\mu}_{\mathbf{X}}, \boldsymbol{\mu}_{\mathbf{Y}(\tilde{\mathbf{r}}_Y)}) = 0,\ k = 1, 2, \cdots, n_e \\
\Pr\{m_l(\mathbf{d}_t, \mathbf{X}, \mathbf{Y}(\tilde{\mathbf{r}}_Y)) < 0\} \ge P_l,\ l = 1, 2, \cdots, n_u \\
\mathbf{d}^L \le \mathbf{d}_t \le \mathbf{d}^U
\end{cases}
\end{cases} \\
\\
\underline{\mathbf{r}}_Y < \tilde{\mathbf{r}}_Y < \overline{\mathbf{r}}_Y \\
g_j(\mathbf{d}_t, \boldsymbol{\mu}_{\mathbf{X}}, \boldsymbol{\mu}_{\mathbf{Y}(\tilde{\mathbf{r}}_Y)}) \le 0,\ j = 1, 2, \cdots, n_j, \\
h_k(\mathbf{d}_t, \boldsymbol{\mu}_{\mathbf{X}}, \boldsymbol{\mu}_{\mathbf{Y}(\tilde{\mathbf{r}}_Y)}) = 0,\ k = 1, 2, \cdots, n_e, \\
\Pr\{m_l(\mathbf{d}_t, \mathbf{X}, \mathbf{Y}(\tilde{\mathbf{r}}_Y)) < 0\} \ge P_l,\ l = 1, 2, \cdots, n_u \\
\mathbf{d}^L \le \mathbf{d} \le \mathbf{d}^U
\end{cases}
\end{cases}
\end{cases}
\tag{21}
$$

The robust design optimization model involves a triple loop procedure.

5.2.3. Model 3— Robust design with both Type I and II imprecise random variables

When both Type I and II imprecise random variables are involved, $\tilde{\mathbf{Y}}$ is given by

$$\tilde{\mathbf{Y}} = [\mathbf{Y}(\tilde{\mathbf{r}}_Y), \mathbf{Y}^{(1)}, \mathbf{Y}^{(2)}, \cdots, \mathbf{Y}^{(n)}], \tilde{\mathbf{r}}_Y \in [\underline{\mathbf{r}}_Y, \overline{\mathbf{r}}_Y] \tag{22}$$

After combining Models 1 and 2, the new robust design optimization model is developed as follows:

$$
\begin{cases}
\min\limits_{\mathbf{d}} R_{\max}(\mathbf{d}) \\
\text{Subject to} \\
R_{\max}(\mathbf{d}) = \max\limits_{\tilde{\mathbf{r}}_Y} r(\mathbf{d}, \tilde{\mathbf{r}}_Y) \\
\quad \begin{cases}
\text{Subject to} \\
r(\mathbf{d}, \tilde{\mathbf{r}}_Y) = \max\{r_t(\mathbf{d}, \tilde{\mathbf{r}}_Y, \mathbf{Y}^{(1)}), r_t(\mathbf{d}, \tilde{\mathbf{r}}_Y, \mathbf{Y}^{(2)}), \cdots, r_t(\mathbf{d}, \tilde{\mathbf{r}}_Y, \mathbf{Y}^{(n_h)})\} \\
r_t(\mathbf{d}, \tilde{\mathbf{r}}_Y, \mathbf{Y}^{(i)}) \\
= C(\mu_Z(\mathbf{d}, \mathbf{X}, \mathbf{Y}(\tilde{\mathbf{r}}_Y), \mathbf{Y}^{(i)}), \sigma_Z(\mathbf{d}, \mathbf{X}, \mathbf{Y}(\tilde{\mathbf{r}}_Y), \mathbf{Y}^{(i)})) \\
\quad - C(\mu_Z(\mathbf{d}_{opt}^{(i)}, \mathbf{X}, \mathbf{Y}(\tilde{\mathbf{r}}_Y), \mathbf{Y}^{(i)}), \sigma_Z(\mathbf{d}_{opt}^{(i)}, \mathbf{X}, \mathbf{Y}(\tilde{\mathbf{r}}_Y), \mathbf{Y}^{(i)})), \forall\, i = 1, 2, \cdots, n_h \\
\quad \begin{cases}
\mathbf{d}_{opt}^{(i)} = \\
\min\limits_{\mathbf{d}_t} C(\mu_Z(\mathbf{d}_t, \mathbf{X}, \mathbf{Y}(\tilde{\mathbf{r}}_Y), \mathbf{Y}^{(i)}), \sigma_Z(\mathbf{d}_t, \mathbf{X}, \mathbf{Y}(\tilde{\mathbf{r}}_Y), \mathbf{Y}^{(i)})) \\
\text{subject to} \\
g_j(\mathbf{d}_t, \boldsymbol{\mu}_{\mathbf{X}}, \boldsymbol{\mu}_{\mathbf{Y}(\tilde{\mathbf{r}}_Y)}, \boldsymbol{\mu}_{\mathbf{Y}^{(i)}}) \le 0,\ j = 1, 2, \cdots, n_j \\
h_k(\mathbf{d}_t, \boldsymbol{\mu}_{\mathbf{X}}, \boldsymbol{\mu}_{\mathbf{Y}(\tilde{\mathbf{r}}_Y)}, \boldsymbol{\mu}_{\mathbf{Y}^{(i)}}) = 0,\ k = 1, 2, \cdots, n_e \\
\Pr\{m_l(\mathbf{d}_t, \mathbf{X}, \mathbf{Y}(\tilde{\mathbf{r}}_Y), \mathbf{Y}^{(i)}) < 0\} \ge P_l,\ l = 1, 2, \cdots, n_u \\
\mathbf{d}^L \le \mathbf{d}_t \le \mathbf{d}^U
\end{cases} \\
\underline{\mathbf{r}}_Y < \tilde{\mathbf{r}}_Y < \overline{\mathbf{r}}_Y \\
g_j(\mathbf{d}, \boldsymbol{\mu}_{\mathbf{X}}, \boldsymbol{\mu}_{\mathbf{Y}(\tilde{\mathbf{r}}_Y)}) \le 0,\ j = 1, 2, \cdots, n_j \\
h_k(\mathbf{d}, \boldsymbol{\mu}_{\mathbf{X}}, \boldsymbol{\mu}_{\mathbf{Y}(\tilde{\mathbf{r}}_Y)}) = 0,\ k = 1, 2, \cdots, n_e \\
\Pr\{m_l(\mathbf{d}, \mathbf{X}, \mathbf{Y}(\tilde{\mathbf{r}}_Y)) < 0\} \ge P_l,\ l = 1, 2, \cdots, n_u \\
\mathbf{d}^L \le \mathbf{d} \le \mathbf{d}^U
\end{cases}
\end{cases}
\tag{23}
$$

It is a quadruple loop problem.

5.3 Numerical procedure

The numerical procedure includes three steps.

Step 1: Perform robust design optimization for every hypothetical distribution and obtain the minimum quality loss.

Step 2: Compute the regrets for design strategies.

Step 3: Identify the maximum regret for design strategies and obtain the optimal design by minimizing the maximum regret.

In the subsequent subsections, the numerical procedures are summarized for models 1, 2, and 3 in details.

5.3.1. Numerical procedure of Model 1

The flowchart for the first robust design optimization model is given in Fig. 6.

Place Fig. 6 here

The main steps are summarized below.

Step 1: Perform robust design optimization for $Z = f(\mathbf{d}, \mathbf{X}, \mathbf{Y}^{(i)})$ using Eq. (19). After the optimization, the minimum quality loss $\mathbf{C_{min}} = [C_{\min}(1), C_{\min}(2), \cdots, C_{\min}(n_h)]$ corresponding to each hypothetical distribution is obtained.

Step 2: Use Eq. (18) to calculate the regret $r(\mathbf{d}, \mathbf{X}, \mathbf{Y}^{(i)})$ for each hypothetical distribution.

Step 3: Identify $R_{\max}(\mathbf{d})$ and minimize it by changing the design variables.

5.3.2. Numerical procedure of Model 2

Fig. 7 shows the flowchart of the numerical procedure.

Place Fig. 7 here

The main steps are described below.

Step 1: Initialize $\mathbf{d}$ and $\tilde{\mathbf{r}}_Y$.

Step 2: Perform the inner loop optimization for the response $Z = f(\mathbf{d}_t, \mathbf{X}, \mathbf{Y}(\tilde{\mathbf{r}}_Y))$ under distribution parameters $\tilde{\mathbf{r}}_Y$.

Step 3: Compute regret $r(\mathbf{d}, \tilde{\mathbf{r}}_Y)$ of design $\mathbf{d}$ with distribution parameters $\tilde{\mathbf{r}}_Y$.

Step 4: Check the convergence. If the regret $r(\mathbf{d}, \tilde{\mathbf{r}}_Y)$ is the maximum, go to next step; otherwise, generate new point for $\tilde{\mathbf{r}}_Y$ and go to step 2.

Step 5: Check convergence. If the maximum regret $R_{\max}$ reaches the minimum, stop; otherwise, generate a new point for $\mathbf{d}$ and go to step 1.

5.3.3. Numerical procedure of Model 3

Fig. 8 depicts the flowchart of the numerical procedure.

Place Fig. 8 here

Similar to Model 2, there are five steps as follows:

Step 1: Initialize $\mathbf{d}$ and $\tilde{\mathbf{r}}_Y$.

Step 2: Solve sub-models i, $i = 1, 2, \cdots, n_h$, and obtain the regrets $r_{temp}(\mathbf{d}, \tilde{\mathbf{r}}_Y, \mathbf{Y}^{(i)})$ with parameters of $\mathbf{d}$ and $\tilde{\mathbf{r}}_Y$.

Step 3: Identify the maximal regret $r(\mathbf{d}, \tilde{\mathbf{r}}_Y)$ from regrets $r_t(\mathbf{d}, \tilde{\mathbf{r}}_Y, \mathbf{Y}^{(i)})$, $i = 1, 2, \cdots, n$.

Step 4: Check convergence. If the regret $r(\mathbf{d}, \tilde{\mathbf{r}}_Y)$ reaches the maximum, go to the next step; otherwise, generate a new point for $\tilde{\mathbf{r}}_Y$ and go to step 2.

Step 5: Check convergence. If the maximum regret $R_{\max}$ is obtained, stop; otherwise, generate a new point for $\mathbf{d}$ and go to step 1.

It is more computationally expensive to perform robust design with imprecise random variables than the design with only precise random variables. Since there are multiple loops involved in the proposed models, solving the models efficiently is a challenging task. For practical applications, the solution is to create meta-models to replace the expensive models that are needed to obtain the objective and constraint functions. The drawback of doing so is the sacrifice of accuracy. Hence there is a tradeoff between efficiency and accuracy. For problems with costly simulation models, constructing meta-models takes most of the time for the robust design. Carefully constructing meta-models is the key to maintaining satisfactory efficiency with acceptable accuracy. Developing more efficient algorithms for robustness assessment will also help improve the efficiency.

6. Robust design optimization of hydrokinetic turbine

In this section, the application of the proposed method in the design of a hydrokinetic turbine system is discussed.

6.1 Problem statement

As one of the most sustainable, clean, and carbon-free energy sources, hydropower has drawn attention of many engineers and researchers (Nitin *et al.* 2011). The most conventional and commonly used way is to construct water dams, which extract energy from running water flow. The construction of water dams, however, has many disadvantages, including the expensive initial construction cost, special requirements for natural sites, and hazards brought to the environment. Hydrokinetic turbine systems and tidal turbine systems have many advantages over water dams (Anyi *et al.* 2010, Lago *et al.* 2010, Hu and Du 2012). Hydrokinetic turbines have the same working principle as that of wind turbines. They are portable; they have a cheap initial construction cost and no special requirements for application sites. Even if many progresses have been made in the area of the design of hydrokinetic turbines, the commercialization of hydrokinetic turbines is still limited by its power efficiency.

One factor that affects the robustness of the power output is the natural variability

of river velocity, which is inherent in the water climate. For instance, a hydrokinetic turbine with a constant rotational speed may have the maximum power efficiency under a certain river velocity. But when the river velocity varies to another level, the efficiency may become low. To maximize the power productivity of a hydrokinetic turbine, the probabilistic characteristics of river velocity should be considered during the design process. One approach to this purpose is the robust design optimization.

The uncertainties involved in the design of hydrokinetic turbines can be classified into two groups – the uncertainty of geometric dimensions due to manufacturing imprecision and the uncertainty in the river velocity. The uncertainty in dimensions is commonly modeled by normal distributions. The distribution parameters can be easily obtained from the nominal dimension variables for the mean values and from the tolerances for standard deviations. It is, however, difficult to obtain the distribution of the river velocity. The data available are not sufficient enough to determine a precise distribution. For the reasons mentioned previously, several candidate distributions for the river velocity may be obtained. There are therefore both precise and imprecise random variables in the design optimization. The proposed new robust design optimization methods can be applied to the optimization of hydrokinetic turbines.

The blades of a hydrokinetic turbine with a constant chord length are shown in Fig. 9. The three-blade system was developed for the potential operation in the Missouri river. The diameter of the hydrokinetic turbine rotor is 1 m. The task of the robust design is to optimize the chord length and rotational speed, which in turn maximize the energy productivity of the turbine.

Place Fig. 9 here

The design variables are therefore the rotational speed ω and the mean of the chord length μ_c. The dimension variables c and r_{root}, which are the chord length and radius of turbine blades, are precise random variables. The imprecise random variable is the river flow velocity v.

6.2 Robust design optimization model for hydrokinetic turbines

6.2.1 Robust design optimization model

Since the river velocity v is an imprecise random variable with multiple hypothetical distributions, Model 1 is applicable to this design problem. The optimization model is given by

$$\begin{cases} \min\limits_{\mathbf{d}=[\mu_c,\,\omega]} R_{\max}(\mu_c, \omega) \\ \text{subject to} \\ R_{\max}(\mu_c, \omega) \\ = \max\{r(\mu_c, \omega, r_{root}, v^{(1)}), r(\mu_c, \omega, r_{root}, v^{(2)}), \cdots, r(\mu_c, \omega, r_{root}, v^{(n_h)})\} \\ r(\mu_c, \omega, r_{root}, v^{(i)}) \\ = C(\mu_{Po}(c, \omega, r_{root}, v^{(i)}), \sigma_{Po}(c, \omega, r_{root}, v^{(i)})) \\ \quad - C(\mu_{Po}(c_{opt}^{(i)}, \omega_{opt}^{(i)}, r_{root}, v^{(i)}), \sigma_{Po}(c_{opt}^{(i)}, \omega_{opt}^{(i)}, r_{root}, v^{(i)})), i = 1, 2, \cdots n_h \\ C(\mu_{Po}, \sigma_{Po}) = k_p[\sigma_{Po}^2 + (\mu_{Po} - T_p)^2] \\ 0.167 \text{ m} \le \mu_c \le 0.25 \text{ m} \\ 2 \text{ rad/s} \le \omega \le 10 \text{ rad/s} \end{cases} \tag{24}$$

where

— n is the number of hypothetical distributions of the river velocity;

— r_{root} is the radius of the hydrokinetic turbine blade;

— $v^{(i)}$ is the i-th hypothetical distribution of the river velocity;

— k_p is the quality loss function coefficient of the power output;

— T_p is the target of the power output;

— $\mu_{Po}(c, \omega, r_{root}, v^{(i)})$ and $\sigma_{Po}(c, \omega, r_{root}, v^{(i)})$ are the mean and standard deviation of the power output, respectively, for the i-th hypothetical distribution of the river velocity;

— $c_{opt}^{(i)}$ and $\omega_{opt}^{(i)}$ are the optimal chord length and rotational speed, respectively, with respect to the i-th hypothetical distribution, which can be obtained by solving the following optimization model:

$$\begin{cases} \min\limits_{\mathbf{d}=[c,\,\omega]} k_p[\sigma_{Po}^2(c, \omega, r_{root}, v^{(i)}) + (\mu_{Po}(c, \omega, r_{root}, v^{(i)}) - T_p)^2] \\ \text{subject to} \\ 0.167 \text{ m} \le c \le 0.25 \text{ m} \\ 2 \text{ rad/s} \le \omega \le 10 \text{ rad/s} \end{cases} \tag{25}$$

The power output is given by

$$Po = 0.5\rho v^3 \pi r_{root}^2 C_p(\lambda, c) \tag{26}$$

where ρ is the river water density (kg/m^3), v is the river velocity (m/s), $C_p(\lambda, c)$ is the power coefficient, and λ is the tip speed ratio of the turbine.

The tip speed ratio λ is given by

$$\lambda = \frac{r_{root}\omega}{v} \tag{27}$$

Substituting Eq. (27) into Eq. (26) yields

$$Po(c, \omega, r_{root}, v) = 0.5\rho v^3 \pi r_{root}^2 C_p(r_{root}\omega / v, c) \tag{28}$$

Eqs. (26)-(28) show that the key to the design is to compute the power coefficient $C_p(\lambda, c)$.

6.2.2 Construction of surrogate model for $C_p(\lambda, c)$

The computational fluid dynamics (CFD) simulation is needed to compute the power coefficient. The CFD simulation, however, is very computationally expensive. It cannot be directly applied to the robust design. Based on the CFD simulations at specified points from design of experiment (DOE), surrogate models were constructed by using the polynomial chaos expansion (PCE) (Xiu and Karniadakis 2003, Xiu and Shen 2009) method for $C_p(\lambda, c)$.

(a) CFD simulation

A CFD analysis was performed to study the effect of operating parameters on the performance of the hydrokinetic turbine. The turbine model used for this study was a 1m radius-constant chord-no twist turbine made from single airfoil SG6043. ANSYS FLUENT was used on an 8 core, 25GB RAM computer. A multiple reference frame technique was employed to model the flow over the turbine, wherein, the turbine was placed within an inner domain, which rotates inside the outer stationary domain (Fig.10 (a)). The fluid flow governing equations were solved in the rotating domain for the inner domain and stationary frame for the outer domain. The transformation of the flow variables took place at the interface between the two domains. Fig. 10 (a) shows various boundary conditions imposed on the CFD model. The velocity inlet boundary condition was specified at the inlet of the outer flow domain while pressure outlet boundary condition was specified at the exit. The outer cylinder surface was modeled as a symmetry boundary so that there is no flux and flow across the boundary. The turbine was treated as a solid wall, and the common region between the two domains was defined as interior through which flow transfer takes place.

Place Fig. 10 here

The flow domain consists of about 2.8 million tetrahedral/hybrid elements. The mesh for boundary layer near the turbine blade surface was locally refined to accurately simulate the near wall boundary layer flow field (Fig. 10b).

A second order discretization scheme was used to solve the convective terms in the fluid flow governing equations. The pressure velocity coupling was solved using the SIMPLE (Semi-implicit method for pressure linked equation) algorithm. The PRESTO (pressure staggering options) scheme was adopted due to its superiority for flows with steep pressure gradient such as the present case (Ansys). A k-ω SST turbulence model of Menter (Menter 1994) was used to characterize the turbulent

flow around the turbine. The convergence criteria for residuals of continuity, momentum, turbulent kinetic energy (k) and specific dissipation (ω) equations were set to 10^{-4} RMS. The fluid domain mesh (Fig. 10) was generated using ANSYS meshing tool, and the grid resolution requirements were well established by keeping $y^+ \sim 120$, so that the wall boundary layer was adequately resolved with good accurate. The procedure and results of the CFD analysis are discussed in details in (Subhra Mukherji *et al.* 2011).

Table 1 presents various parameters chosen for the CFD analysis while Table 2 summarizes the results of the CFD analysis for the constant chord turbines used for the robust design study. Various parameters, such as the tip speed ratio (TSR) and chord length (c), were tested to quantify their effect on the performance of the hydrokinetic turbine. The CFD simulations were carried out for turbines with chord length varying from 0.167 to 0.3m and TSR varying from 1.5 to 4.

Place Tables 1-2 here

(b) Polynomial Chaos Expansion method

The expansion order for the PCE is three, the expansion interval of the tip speed ratio is [1.5, 4.0], and the interval of the chord length is [0.167, 0.25] m. The constructed surrogate model is given by

$$\begin{aligned}\hat{C}_p(\xi_1,\xi_2) &= \sum_{k=0}^{9} \chi_k \Gamma_k(\xi) \\ &= \chi_0 + \sum_{i=1}^{2} \chi_i L_1(\xi_i) + \chi_3 L_1(\xi_1) L_1(\xi_2) + \sum_{i=1}^{2} \chi_{3+i} L_2(\xi_i) \\ &\quad + \chi_6 L_2(\xi_1) L_1(\xi_2) + \chi_7 L_1(\xi_1) L_2(\xi_2) + \sum_{i=1}^{2} \chi_{7+i} L_3(\xi_i)\end{aligned} \tag{29}$$

where

$$\xi_1 = \frac{2\lambda - L_\lambda - U_\lambda}{U_\lambda - L_\lambda} \tag{30}$$

$$\xi_2 = \frac{2c - L_c - U_c}{U_c - L_c} \tag{31}$$

in which U_λ and L_λ are the upper and lower bounds of the tip speed ratio expansion interval, respectively; U_c and L_c are the upper and lower bounds of the chord length expansion interval, respectively; $L_i(\cdot)$ is the i-th order Legendre polynomial basis. For $i = 1$, $L_1(x) = x$; for $i = 2$, $L_2(x) = \frac{1}{2}(3x^2 - 1)$; and for $i = 3$,

$L_3(x) = \frac{1}{2}(5x^3 - 3x)$. The Legendre polynomial bases were selected to perform the chaos expansion because the design variables can be treated as generalized variables with uniform distributions and they have equal weights over the expansion intervals.

To compute coefficients $\chi_k, k = 0, 1, 2, \cdots, 9$, or the PCE, the point collocation method was employed (Wei *et al.* 2008, Eldred and Burkardt 2009, Hu and Youn 2011). Three-dimensional CFD simulations were performed first at the sample points generated from design of experiments (DOE). Based on the results of the CFD simulations, the power coefficients of the turbine blades were obtained. With N_p CFD simulations, the coefficients χ_k were solved with the following equation:

$$\begin{pmatrix} \Gamma_0(\xi^1) & \Gamma_1(\xi^1) & \cdots & \Gamma_9(\xi^1) \\ \Gamma_0(\xi^2) & \Gamma_1(\xi^2) & \cdots & \Gamma_9(\xi^2) \\ \vdots & \vdots & \cdots & \vdots \\ \Gamma_0(\xi^{N_p}) & \Gamma_1(\xi^{N_p}) & \cdots & \Gamma_9(\xi^{N_p}) \end{pmatrix} \begin{pmatrix} \chi_0^s \\ \chi_1^s \\ \vdots \\ \chi_9^s \end{pmatrix} = \begin{pmatrix} C_p(\xi^1) \\ C_p(\xi^2) \\ \vdots \\ C_p(\xi^{N_p}) \end{pmatrix} \tag{32}$$

where $\xi^i = [\xi_1^i, \xi_2^i], i = 1, \cdots, N_p$, is the *i*-th group of sample points, and $C_p(\xi^i)$ is the power coefficient with the *i*-th group of sample points obtained from the CFD simulations. The coefficients are given by

$$\begin{aligned} &\chi_0 = 0.1048,\ \chi_1 = 0.0091,\ \chi_2 = 0,\ \chi_3 = -0.0171,\ \chi_4 = -0.0262,\ \chi_5 = -0.0035, \\ &\chi_6 = 0.0059,\ \chi_7 = 2.659 \times 10^{-4},\ \chi_8 = -0.0019,\ \chi_9 = -0.0090 \end{aligned} \tag{33}$$

After the construction of surrogate model, the goodness-of-fit was evaluated by calculating the coefficients of determination. The coefficients of determination R^2 are given by

$$R^2 = 1 - \frac{\sum (C_p - \bar{C}_p)^2}{\sum (C_p - \hat{C}_p(\xi))^2} \tag{34}$$

where C_p is the data obtained from the CFD simulations, $\bar{C}_p$ is the mean of all data from the CFD simulations, and $\hat{C}_p(\xi)$ is the data computed from the surrogate model. R^2 is 0.9370, which indicates that the fitted model is accurate. (A coefficient of determination of 0.9 or higher is considered as a good fitting).

Fig. 11 plots the scatter diagram of the results obtained from the CFD simulations and the surrogate model. The diagram shows that the points are evenly distributed at the two sides of $C_p = \hat{C}_p$. It indicates that the surrogate model obtained in Eq. (29) can accurately describe the relationship between power coefficient, TSR, and chord length.

Place Fig. 11 here

Fig. 12 presents the surrogate model of the power coefficient and data points obtained from the CFD simulations. The shaded surface is the surrogate model, while the star points represent the data from the CFD simulations.

Place Fig. 12 here

All the equations for calculating the power output $Po(c, \omega, r_{root}, v)$ are now available. With the surrogate model for the power coefficient C_p, it is computaionally cheap to compute $Po(c, \omega, r_{root}, v)$. The MCS method can therefore be applied to the computation of the mean and standard deviation of $Po(c, \omega, r_{root}, v)$, which are needed by Eqs. (24) and (25). With MCS, the mean and standard deviation are computed by

$$\mu_{Po}(c, \omega, r_{root}, v^{(j)}) = \frac{1}{N}\sum_{i=1}^{N} Po(c_i, \omega, r_{root,i}, v_i^{(j)}) \tag{35}$$

$$\sigma_{Po}(c, \omega, r_{root}, v^{(j)}) = \sqrt{\frac{1}{N-1}\sum_{i=1}^{N}[Po(c_i, \omega, r_{root,i}, v_i^{(j)}) - \mu_{Po}(c, \omega, r_{root}, v^{(j)})]^2} \tag{36}$$

where c_i, $r_{root,i}$, and $v_i^{(j)}$ are *i*-th sample of c, r_{root}, and $v^{(j)}$, respectively.

6.3 Data

Table 3 presents the precise parameters and random variables for the design optimization of the hydrokinetic turbine. Amongst these parameters, r_{root} and c are truncated at three sigma level due to the manufacturing tolerance, and the river velocity v is truncated at 0.8 m/s and 4.5 m/s because of the cut-in and cut-out river velocities.

Place Table 3 here

The river velocity v can be obtained from the historical river velocity data (as shown in Fig. 13) of Missouri river from year of 1898 to 1989.

Place Fig. 13 here

Before fitting distributions for the historical data, the Lilliefors test is performed, which is a special case of the Kolmogorov-Smirnov goodness-of-fit test. The Lilliefors test tests raw data against normal, lognormal, extreme value, Weibull, and exponential distributions without specifying the distribution parameters. Under the 95% confidence, the normal, lognormal, and Weibull distributions were not rejected, and the extreme value distribution was rejected. The normal, lognormal, and Weibull distributions were then fitted with the data. Fig. 14 shows the velocity data and the three distributions. The associated distribution parameters are given in Table 4.

Place Fig. 14 here

Place Table 4 here

To verify the three distributions, after their fittings, the Kolmogorov–Smirnov tests were performed using the raw data in Fig. 13. All the distribution passed the testing under 95% confidence. This means that the three disrtibutions could serve as cadidate distribution for the river velocity.

6.4 Numerical procedure for the robust design optimization of hydrokinetic turbines

Fig. 15 shows the main steps for the robust design of hydrokinetic turbines.

Place Fig. 15 here

6.5 Results and discussions

Table 5 shows the results from both the robust design optimization with only precise random variables (the traditional method) and the robust design optimization based on the minimax regret criterion (the new method). In this table, Design *i*, where $i = 1, 2, 3$, means the optimal design considering only the *i*-th candidate distribution. The three designs are from the traditional robust design method. The "Optimal Design" in the table stands for the design obtained from the new method with the MMR criterion.

Place Table 5 here

Table 6 gives the means and standard deviations of power outputs of the four designs, and Table 7 provides the quality losses of the four designs.

Place Tables 6-7 here

The two tables clearly show that Design *i* is the optimal for the *i*-th candidate distribution because of the least quality loss, but is not optimal for the other two candidate distributions. For example, when Design 1 is adopted, for the Weibull distribution, the loss is $\$4.72\times10^7$, which is the minimum amongst the four designs. If the distribution is indeed Weibull, Design 1 is then the true optimal design. However, if the true distribution is Lognormal, the quality loss will be $\$2.93\times10^7$, and the minimal loss will be $\$2.6685\times10^7$ from Design 2; if the true distribution is Normal, the quality loss will be $\$4.5891\times10^7$, and the minimal loss will be $\$4.5875\times10^7$ from Design 3. Then Design 1 will no longer be optimal for these two situations, for which nonzero regret values will be generated. The regret values for Design 1 are calculated as follows:

For the Weibull distribution,

$$\begin{aligned}&\text{Quality loss of Design 1} - \text{Minimal quality loss under this distribution}\\ &= \$4.72\times10^7 - \$4.72\times10^7 = \$0\end{aligned}$$

Similarly, for the Lognormal distribution,

$$\$2.93\times10^{7}-\$2.67\times10^{7}=\$2.59\times10^{6}$$

For the normal distribution,

$$\$4.59\times10^{7}-\$4.58\times10^{7}=\$0.016\times10^{6}$$

Thus, Design 1 has a maximum regret of $\$2.59\times10^{6}$. Similarly, the regret values for Design 2, 3, and the optimal design can be calculated. All the regret values of the four designs are shown in Table 9 and plotted in Fig. 16. In Table 8, the maximum regrets of the four designs are summarized. The maximum regrets for Design 1, 2, 3, and the optimal design are $\$2.5904\times10^{6}$, $\$3.1243\times10^{6}$, $\$2.2281\times10^{6}$, and $\$0.6948\times10^{6}$, respectively.

The results show that the maximum regrets of the three designs obtained from the traditional robust design method is about three times of that of the optimal design. It indicates that the robust design method based on the MMR criterion has improved the robustness of the design with respect to the uncertainties in the random variables.

Place Table 8 here

Place Fig. 16 here

---

7. Conclusions

In many engineering applications, some random variables are precisely known and others may be imprecisely known. There are uncertainties in both of the probabilistic models and probabilistic parameters of random variable due to the incomplete information or limited data for the modeling of random variable. The results of design optimizations would be affected by the model used for the imprecise random variable. To make the design more robust against the uncertainties in random variables, a robust design method based on the MMR criterion is developed. The method is able to minimize the maximum regret of the design with respect to the quality loss. The robust design method with only precise random variable, the

Taguchi quality loss function, and the MMR criterion are considered together to get an optimal design.

The new method has been applied to the robust design optimization of a hydrokinetic turbine. The result demonstrates that the traditional robust design can introduce large regrets in the quality loss if imprecise random variables exist. The result also shows that the new method can reduce the regret significantly.

The application was based on the Monte Carlo simulation, which needs to call the objective and constraint functions many times. For applications with expensive functions, solving the robust design optimization will be less efficient. Improving the efficiency will be one of the future research directions.

Acknowledgement

The authors gratefully acknowledge the support from the Office of Naval Research through contract ONR N000141010923 (Program Manager - Dr. Michele Anderson) and the Intelligent Systems Center at the Missouri University of Science and Technology.

Reference

Ahmad, R. and Kamaruddin, S., 2012. An overview of time-based and condition-based maintenance in industrial application. *Computers and Industrial Engineering,* 63 (1), 135-149.

Ansys, *Fluent 12.0 User's Guide, Ansys Inc. 2009,*

Anyi, M., Kirke, B. and Ali, S., 2010. Remote community electrification in sarawak, malaysia. *Renewable Energy,* 35 (7), 1609-1613.

Aughenbaugh, J.M. and Paredis, C.J.J., 2006. The value of using imprecise probabilities in engineering design. *Journal of Mechanical Design, Transactions of the ASME,* 128 (4), 969-979.

Baillie, M., Azzopardi, L. and Ruthven, I., 2008. Evaluating epistemic uncertainty under incomplete assessments. *Information Processing and Management,* 44 (2), 811-837.

Banerjee, B. and Smith, B.G., 2011. Reliability analysis for inserts in sandwich composites. *Advanced Materials Research,* 275, 234-238.

Chang, N.B. and Davila, E., 2007. Minimax regret optimization analysis for a regional solid waste management system. *Waste Management,* 27 (6), 820-832.

Chen, W., Wiecek, M.M. and Zhang, J., 1999. Quality utility - a compromise programming approach to robust design. *Journal of Mechanical Design, Transactions of the ASME,* 121 (2), 179-187.

Choi, H., Mcdowell, D.L., Allen, J.K., Rosen, D. and Mistree, F., 2008. An inductive design exploration method for robust multiscale materials design. *Journal of Mechanical Design, Transactions of the ASME,* 130 (3)

Conde, E. and Candia, A., 2007. Minimax regret spanning arborescences under

uncertain costs. *European Journal of Operational Research,* 182 (2), 561-577.

Cross, R., Makeev, A. and Armanios, E., 2007. Simultaneous uncertainty quantification of fracture mechanics based life prediction model parameters. *International Journal of Fatigue,* 29 (8), 1510-1515.

Dolšek, M., 2012. Simplified method for seismic risk assessment of buildings with consideration of aleatory and epistemic uncertainty. *Structure and Infrastructure Engineering,* 8 (10), 939-953.

Du, X., 2008. Unified uncertainty analysis by the first order reliability method. *Journal of Mechanical Design, Transactions of the ASME,* 130 (9), 0914011-09140110.

Du, X., 2012. Reliability-based design optimization with dependent interval variables. *International Journal for Numerical Methods in Engineering,* 91 (2), 218-228.

Du, X. and Chen, W., 2000. Methodology for managing the effect of uncertainty in simulation-based design. *AIAA journal,* 38 (8), 1471-1478.

Du, X. and Chen, W., 2002. Efficient uncertainty analysis methods for multidisciplinary robust design. *AIAA Journal,* 40 (3), 545-552.

Du, X., Sudjianto, A. and Huang, B., 2005. Reliability-based design with the mixture of random and interval variables. *Journal of Mechanical Design, Transactions of the ASME,* 127 (6), 1068-1076.

Dubey, A.K. and Yadava, V., 2008. Robust parameter design and multi-objective optimization of laser beam cutting for aluminium alloy sheet. *International Journal of Advanced Manufacturing Technology,* 38 (3-4), 268-277.

Eldred, M.S. and Burkardt, J., Year. Comparison of non-intrusive polynomial chaos and stochastic collocation methods for uncertainty quantificationed.^eds. *47th AIAA Aerospace Sciences Meeting including the New Horizons Forum and Aerospace Exposition , art. no. 2009-0976*

He, Y., 2009. Surface wind speed probability distribution in the southeast pacific of marine stratus and stratocumulus regions. *Central European Journal of Geosciences,* 1 (4), 443-455.

Herrmann, J.W., 2009. Design optimization with imprecise random variables. *SAE International Journal of Materials and Manufacturing,* 2 (1), 99-107.

Hu, C. and Youn, B.D., 2011. Adaptive-sparse polynomial chaos expansion for reliability analysis and design of complex engineering systems. *Structural and Multidisciplinary Optimization,* 43 (3), 419-442.

Hu, Z. and Du, X., 2012. Reliability analysis for hydrokinetic turbine blades. *Renewable Energy,* 48, 251-262.

Hu, Z., Li, H., Du, X. and Chandrashekhara, K., 2012. Simulation-based time-dependent reliability analysis for composite hydrokinetic turbine blades. *Structural and Multidisciplinary Optimization,* 1-17.

Huang, B. and Du, X., 2008. Probabilistic uncertainty analysis by mean-value first order saddlepoint approximation. *Reliability Engineering and System Safety,* 93 (2), 325-336.

Huang, H.Z. and Zhang, X., 2009. Design optimization with discrete and continuous variables of aleatory and epistemic uncertainties. *Journal of Mechanical*

Design, Transactions of the ASME, 131 (3), 0310061-0310068.

Inuiguchi, M. and Kume, Y., 1991. Goal programming problems with interval coefficients and target intervals. *European Journal of Operational Research,* 52 (3), 345-360.

Inuiguchi, M. and Sakawa, M., 1995. Minimax regret solution to linear programming problems with an interval objective function. *European Journal of Operational Research,* 86 (3), 526-536.

Jiang, C., Han, X., Li, W.X., Liu, J. and Zhang, Z., 2012. A hybrid reliability approach based on probability and interval for uncertain structures. *Journal of Mechanical Design, Transactions of the ASME,* 134 (3)

Karpel, M., Moulin, B. and Idan, M., 2003. Robust aeroservoelastic design with structural variations and modeling uncertainties. *Journal of Aircraft,* 40 (5), 946-954.

Kim, D.W., Jung, S.S., Sung, Y.H. and Kim, D.H., 2011. Optimization of smes windings utilizing the first-order reliability method. *Transactions of the Korean Institute of Electrical Engineers,* 60 (7), 1354-1359.

Lago, L.I., Ponta, F.L. and Chen, L., 2010. Advances and trends in hydrokinetic turbine systems. *Energy for Sustainable Development,* 14 (4), 287-296.

Li, Y. and Huang, G.H., 2009. Inexact minimax regret integer programming for long-term planning of municipal solid waste management - part b: Application. *Environmental Engineering Science,* 26 (1), 219-234.

Li, Y.P. and Huang, G.H., 2006. Minimax regret analysis for municipal solid waste management: An interval-stochastic programming approach. *Journal of the Air and Waste Management Association,* 56 (7), 931-944.

Li, Y.P., Huang, G.H. and Nie, S.L., 2009. A robust interval-based minimax-regret analysis approach for the identification of optimal water-resources-allocation strategies under uncertainty. *Resources, Conservation and Recycling,* 54 (2), 86-96.

Lu, X. and Li, H.X., 2009. Perturbation theory based robust design under model uncertainty. *Journal of Mechanical Design, Transactions of the ASME,* 131 (11), 1110061-1110069.

Lu, X.J., Li, H.X. and Chen, C.L.P., 2010. Variable sensitivity-based deterministic robust design for nonlinear system. *Journal of Mechanical Design, Transactions of the ASME,* 132 (6), 0645021-0645027.

Madsen, H.O., Krenk, S., Lind, N.C., 1986. *Methods of structural safety* New Jersey: Englewood Cliffs.

Makeev, A., Nikishkov, Y. and Armanios, E., 2007. A concept for quantifying equivalent initial flaw size distribution in fracture mechanics based life prediction models. *International Journal of Fatigue,* 29 (1), 141-145.

Manski, C.F., 2007. Minimax-regret treatment choice with missing outcome data. *Journal of Econometrics,* 139 (1), 105-115.

Maymon, G., 2005. Probabilistic crack growth behavior of aluminum 2024-t351 alloy using the 'unified' approach. *International Journal of Fatigue,* 27 (7), 828-834.

Mcgill, B.J., Maurer, B.A. and Weiser, M.D., 2006. Empirical evaluation of neutral

theory. *Ecology,* 87 (6), 1411-1423.

Menter, F.R., 1994. Two-equation eddy-viscosity turbulence models for engineering applications. *AIAA Journal,* 32 (8), 1598-1605.

Millwater, H. and Feng, Y., 2011. Probabilistic sensitivity analysis with respect to bounds of truncated distributions. *Journal of Mechanical Design, Transactions of the ASME,* 133 (6)

Morgan, E.C., Lackner, M., Vogel, R.M. and Baise, L.G., 2011. Probability distributions for offshore wind speeds. *Energy Conversion and Management,* 52 (1), 15-26.

Nikolaidis, E. and Mourelatos, Z.P., 2011. Imprecise reliability assessment when the type of the probability distribution of the random variables is unknown. *International Journal of Reliability and Safety,* 5 (2), 140-157.

Nitin, K., Suchi, S.M. and Arindam, B., Year. Numerical modeling and optimization of hydrokinetic turbine. *In*: Esfuelcell2011, ed.^eds. *Proceedings of ASME 2011 5th International Conference on Energy Sustainability & 9th Fuel Cell Science, Engineering and Technology Conference*, Washington, DC: ASME.

Papadimitriou, D.I. and Giannakoglou, K.C., 2012. Third-order sensitivity analysis for robust aerodynamic design using continuous adjoint. *International Journal for Numerical Methods in Fluids,*

Radaev, N.N., 2000. An increase in the accuracy of prediction of disasters by accounting for inhomogeneous data on a damage. *Automation and Remote Control,* 61 (3 PART 2), 530-536.

Ramakrishnan, B. and Rao, S.S., 1996. A general loss function based optimization procedure for robust design. *Engineering Optimization,* 25 (4), 255-276.

Renou, L. and Schlag, K.H., 2010. Minimax regret and strategic uncertainty. *Journal of Economic Theory,* 145 (1), 264-286.

Renou, L. and Schlag, K.H., 2011. Implementation in minimax regret equilibrium. *Games and Economic Behavior,* 71 (2), 527-533.

Ruderman, A., Choi, S.K., Patel, J., Kumar, A. and Allen, J.K., 2010. Simulation-based robust design of multiscale products. *Journal of Mechanical Design, Transactions of the ASME,* 132 (10)

Saha, A. and Ray, T., 2011. Practical robust design optimization using evolutionary algorithms. *Journal of Mechanical Design, Transactions of the ASME,* 133 (10)

Stoye, J., 2011. Statistical decisions under ambiguity. *Theory and Decision,* 70 (2), 129-148.

Stoye, J., 2012. Minimax regret treatment choice with covariates or with limited validity of experiments. *Journal of Econometrics,* 166 (1), 138-156.

Subhra Mukherji, S., Kolekar, N., Banerjee, A. and Mishra, R., 2011. Numerical investigation and evaluation of optimum hydrodynamic performance of a horizontal axis hydrokinetic turbine. *Journal of Renewable and Sustainable Energy,* 3 (6)

Taguchi, G., 1993. Taguchi on robust technology development: Bringing quality engineering upstream. *ASME Press, New York,* 1–14.

Taguchi, G., Chowdhury, S. and Taguchi, S., 2000. Robust engineering. *McGraw Hill, New York,* , 1–10.

Tetenov, A., 2012. Statistical treatment choice based on asymmetric minimax regret criteria. *Journal of Econometrics,* 166 (1), 157-165.

Tsui, K.-L., 1992. An overview of taguchi method and newly developed statistical methods for robust design. *IIE Transactions,* 24 (5), 44-57.

Utkin, L.V., 2004. An uncertainty model of structural reliability with imprecise parameters of probability distributions. *ZAMM Zeitschrift fur Angewandte Mathematik und Mechanik,* 84 (10-11), 688-699.

Veneziano, D., Agarwal, A. and Karaca, E., 2009. Decision making with epistemic uncertainty under safety constraints: An application to seismic design. *Probabilistic Engineering Mechanics,* 24 (3), 426-437.

Walley, P., 1991. Statistical reasoning with imprecise probabilities. *Chapman and Hall, New York,,*

Wei, D.L., Cui, Z.S. and Chen, J., 2008. Uncertainty quantification using polynomial chaos expansion with points of monomial cubature rules. *Computers and Structures,* 86 (23-24), 2102-2108.

Weichselberger, K., 2000. The theory of interval-probability as a unifying concept for uncertainty. *International Journal of Approximate Reasoning,* 24 (2-3), 149-170.

Wiebenga, J.H., Van Den Boogaard, A.H. and Klaseboer, G., 2012. Sequential robust optimization of a v-bending process using numerical simulations. *Structural and Multidisciplinary Optimization,* 46 (1), 137-153.

Xiu, D. and Karniadakis, G.E., 2003. Modeling uncertainty in flow simulations via generalized polynomial chaos. *Journal of Computational Physics,* 187 (1), 137-167.

Xiu, D. and Shen, J., 2009. Efficient stochastic galerkin methods for random diffusion equations. *Journal of Computational Physics,* 228 (2), 266-281.

Youn, B.D., Choi, K.K., Du, L. and Gorsich, D., 2007. Integration of possibility-based optimization and robust design for epistemic uncertainty. *Journal of Mechanical Design, Transactions of the ASME,* 129 (8), 876-882.

Zhang, J. and Du, X., 2010. A second-order reliability method with first-order efficiency. *Journal of Mechanical Design, Transactions of the ASME,* 132 (10)

Zhang, M., 2011. Two-stage minimax regret robust uncapacitated lot-sizing problems with demand uncertainty. *Operations Research Letters,* 39 (5), 342-345.

Zhang, R. and Mahadevan, S., 2000. Model uncertainty and bayesian updating in reliability-based inspection. *Structural Safety,* 22 (2), 145-160.

List of Table Captions

Table 1 Parameters for CFD analysis

Table 2 Results of CFD simulations

Table 3 Precise parameters and random variables

Table 4 Hypothetical distributions for river velocity

Table 5 Optimized results of design variables

Table 6 Means and standard deviations of power output

Table 7 Quality losses of different designs under candidate distributions

Table 8 Regret values of the four designs under hypothetical distributions

List of Figure Captions

Figure 1 CDF of a random variable with three possible distributions

Figure 2 CDFs of $\tilde{Y}$ with imprecise mean

Figure 3 CDFs of $\tilde{Y}$ with imprecise standard deviation

Figure 4 CDFs of $\tilde{Y}$ with imprecise mean and standard deviation

Figure 5 PDFs of Z before and after robust design optimization

Figure 6 Flowchart of the first robust design optimization model

Figure 7 Flowchart of the second robust design optimization model

Figure 8 Flowchart of the third robust design optimization model

Figure 9 Prototype of a Hydrokinetic turbine

Figure 10 Boundary conditions for 3D CFD model and CFD mesh-Local refinement

Figure 11 Scatter diagram of the results obtained from CFD simulations and response surface model

Figure 12 Surrogate model of the power coefficient and data points from simulations

Figure 13 Historical river velocity data of Missouri river at Hermann, Missouri station

Figure 14 Fitted distributions for the river velocity

Figure 15 Flowchart of robust design of hydrokinetic turbine

Figure 16 Regret values of four different designs under different candidate distributions

Table 1. Parameters for CFD analysis

Hydrofoil	SG-6043
Density (ρ)	998.2 kg/m^3
Pressure (p)	101.3 kPa
Rotor radius (R)	1 m
Chord length (c)	0.167-0.3
Number of blades (N)	2-4
Blade pitch (θ_P)	10°
Rotor speed (Ω)	3-8 rad/s
Fluid speed (U_∞)	2 m/s
Turbulence model	k-ω SST
Interpolating scheme	2nd order upwind
Pressure scheme	PRESTO
Residual error	1×10^{-4}

Table 2. Results of CFD simulations

c(m)	0.167	0.2	0.25
TSR	C_p	C_p	C_p
1.5	0.06	0.06	0.08
2	0.09	0.10	0.10
2.5	0.12	0.12	0.11
3	0.13	0.16	0.10
3.5	0.14	0.12	0.08
4	0.10	0.08	0.07

Table 3. Precise parameters and random variables

Variable	ρ	r_{root}	c	k_p	T_p
Type	Constant	Truncated normal	Truncated normal	Constant	Constant
Mean	1×10^{3} kg/m^{3}	1 m	μ_c	2	6000
Standard deviation	N/A	1×10^{-2} m	1×10^{-3} m	N/A	N/A

Table 4. Hypothetical distributions for river velocity

Distribution Type	Weibull (Distribution 1)	Lognormal (Distribution 2)	Normal (Distribution 3)
Distribution Parameters	1.85 (Scale)	1.77 m/s (Mean)	1.82 m/s (Mean)
	14.17 (Shape)	0.13 m/s (Std)	0.14 m/s (Std)

where Std stands for a standard deviation.

Table 5. Optimized results of design variables

	Design 1	Design 2	Design 3	Optimal Design
Rotational speed (r/min)	48.56	61.91	49.55	54.95
Chord (m)	0.2223	0.2218	0.2222	0.2230

Table 6. Means and standard deviations of power output ($\times 10^3$ W)

Candidate distributions		Design 1	Design 2	Design 3	Optimal Design
Weibull	Mean	1.1488	0.9961	1.1483	1.1157
	Std	0.2879	0.3749	0.2943	0.3298
Lognormal	Mean	2.1789	2.3502	2.1997	2.3024
	Std	0.1169	0.1446	0.1191	0.1309
Normal	Mean	1.2177	1.0863	1.2189	1.1950
	Std	0.2742	0.3579	0.2805	0.3147

Table 7. Quality losses of different designs under candidate distributions ($\times 10^7$ \$)

Hypothetical distributions	Design 1	Design 2	Design 3	Optimal Design
Weibull	4.7235	5.0389	4.7250	4.7930
Lognormal	2.9275	2.6685	2.8913	2.7379
Normal	4.5891	4.8545	4.5875	4.6375

Table 8. Regret values of the four designs under hypothetical distributions ($\times 10^6$ \$)

Hypothetical distributions	Design 1	Design 2	Design 3	Optimal Design
Weibull	0	3.1243	0.0156	0.6948
Lognormal	2.5904	0	2.2281	0.6948
Normal	0.0155	2.6701	0	0.4995
Maximum regret	2.5904	3.1243	2.2281	0.6948

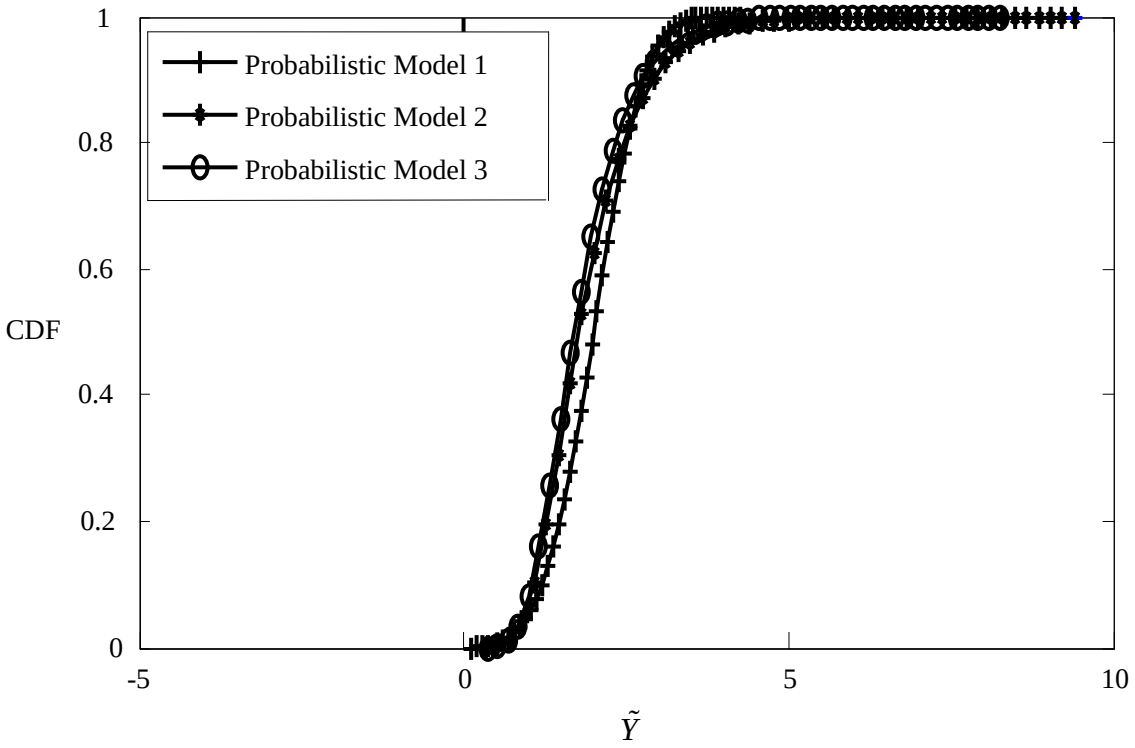

Fig. 1. CDF of a random variable with three possible distributions

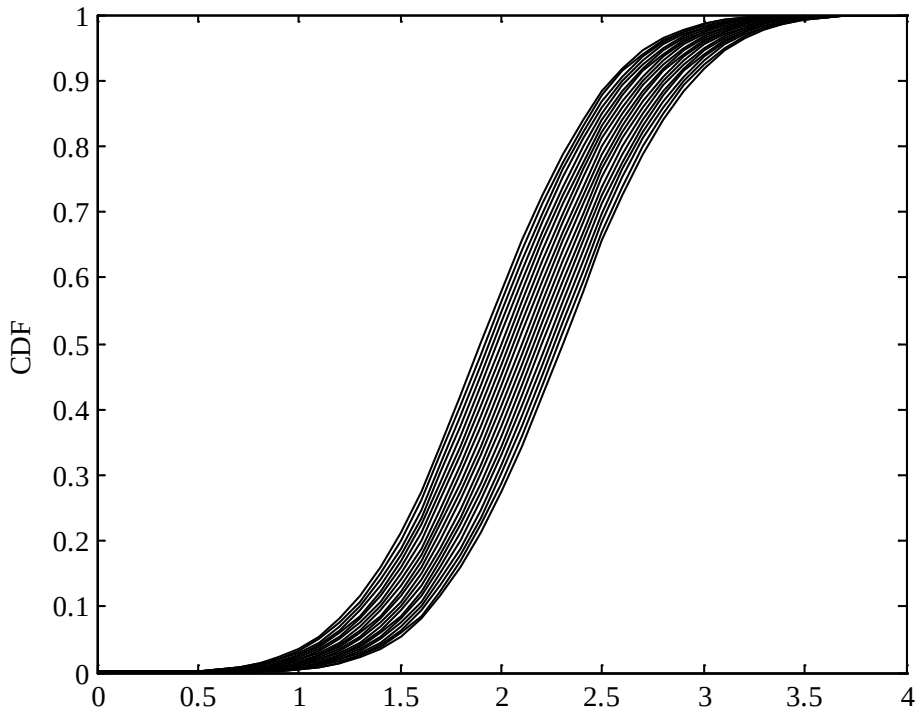

Fig. 2. CDFs of $\tilde{Y}$ with imprecise mean

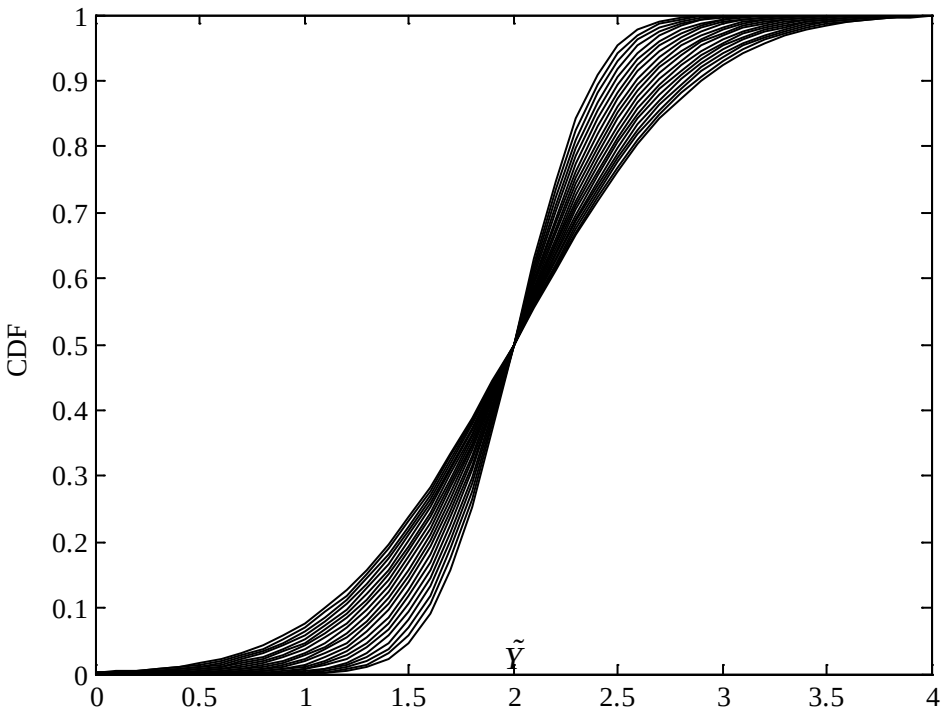

Fig. 3. CDFs of $\tilde{Y}$ with imprecise standard deviation

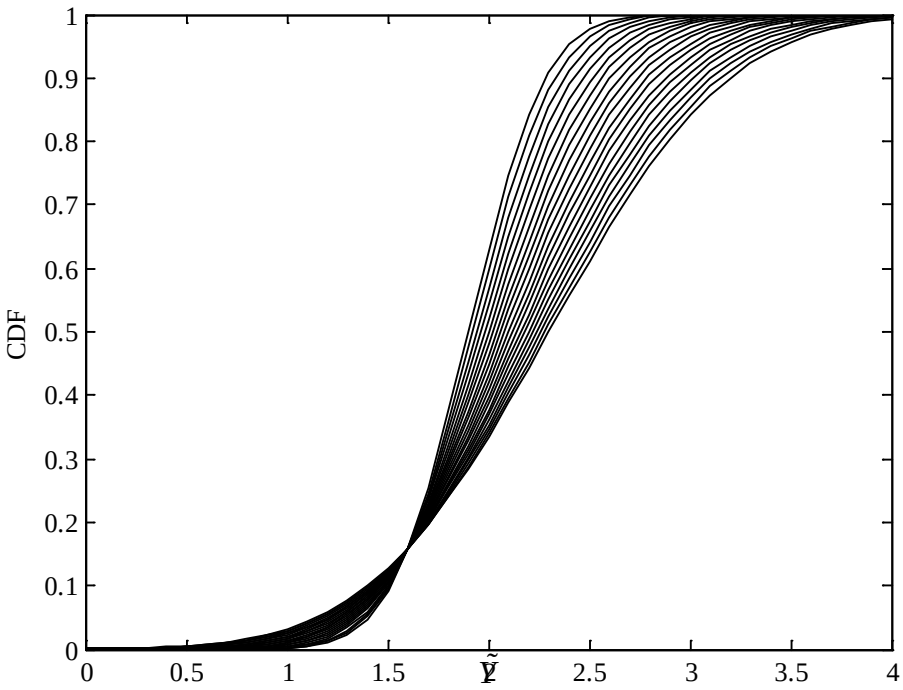

Fig. 4. CDFs of $\tilde{Y}$ with imprecise mean and standard deviation

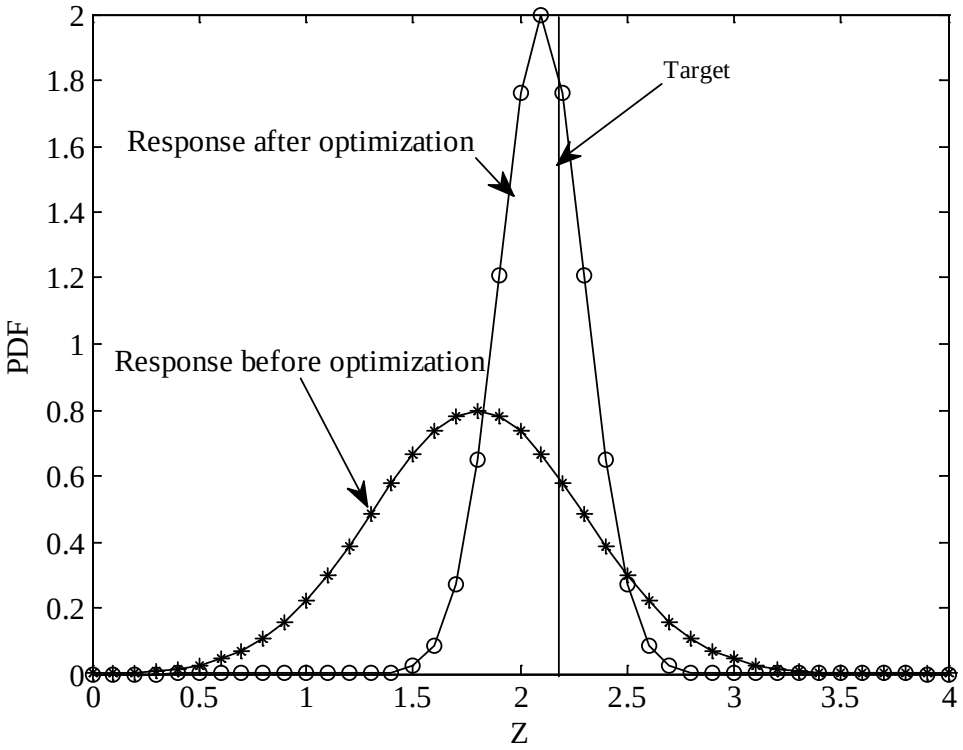

Fig. 5. PDFs of Z before and after robust design optimization

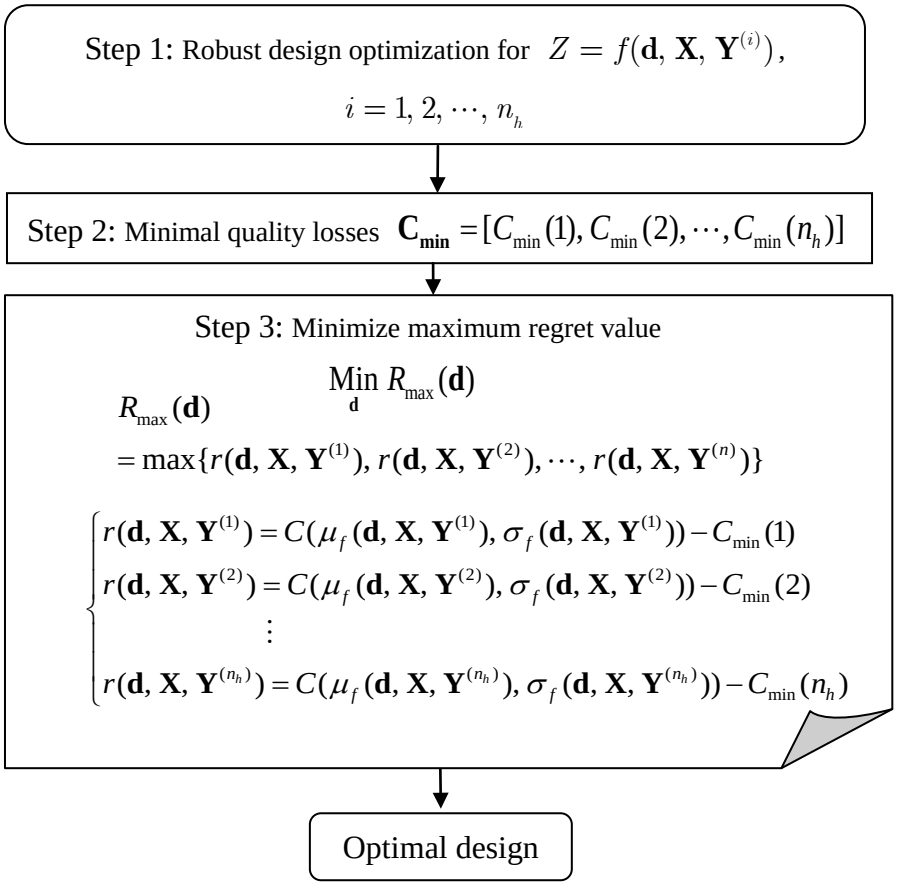

Fig. 6. Flowchart of the first robust design optimization model

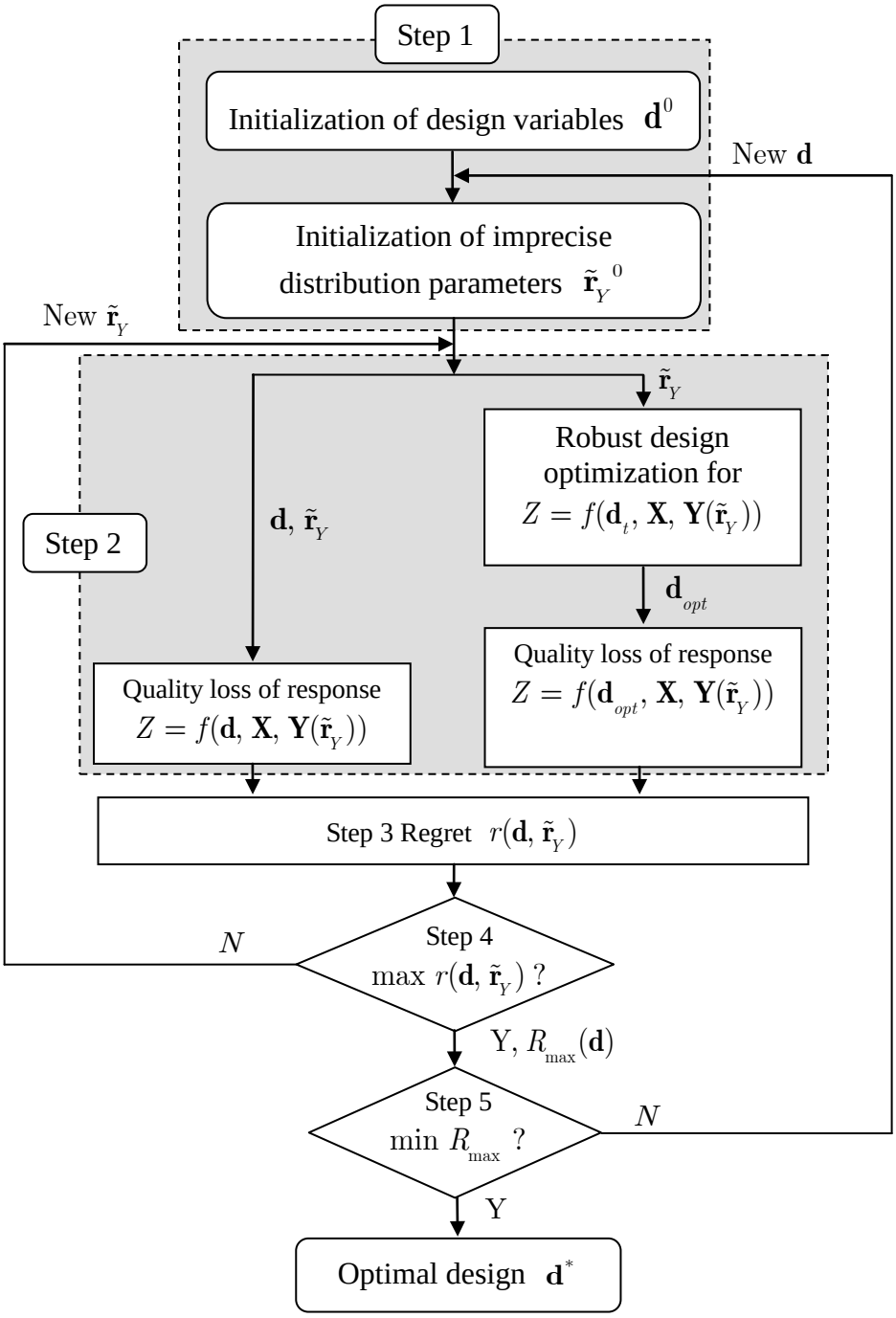

Fig. 7. Flowchart of the second robust design optimization model

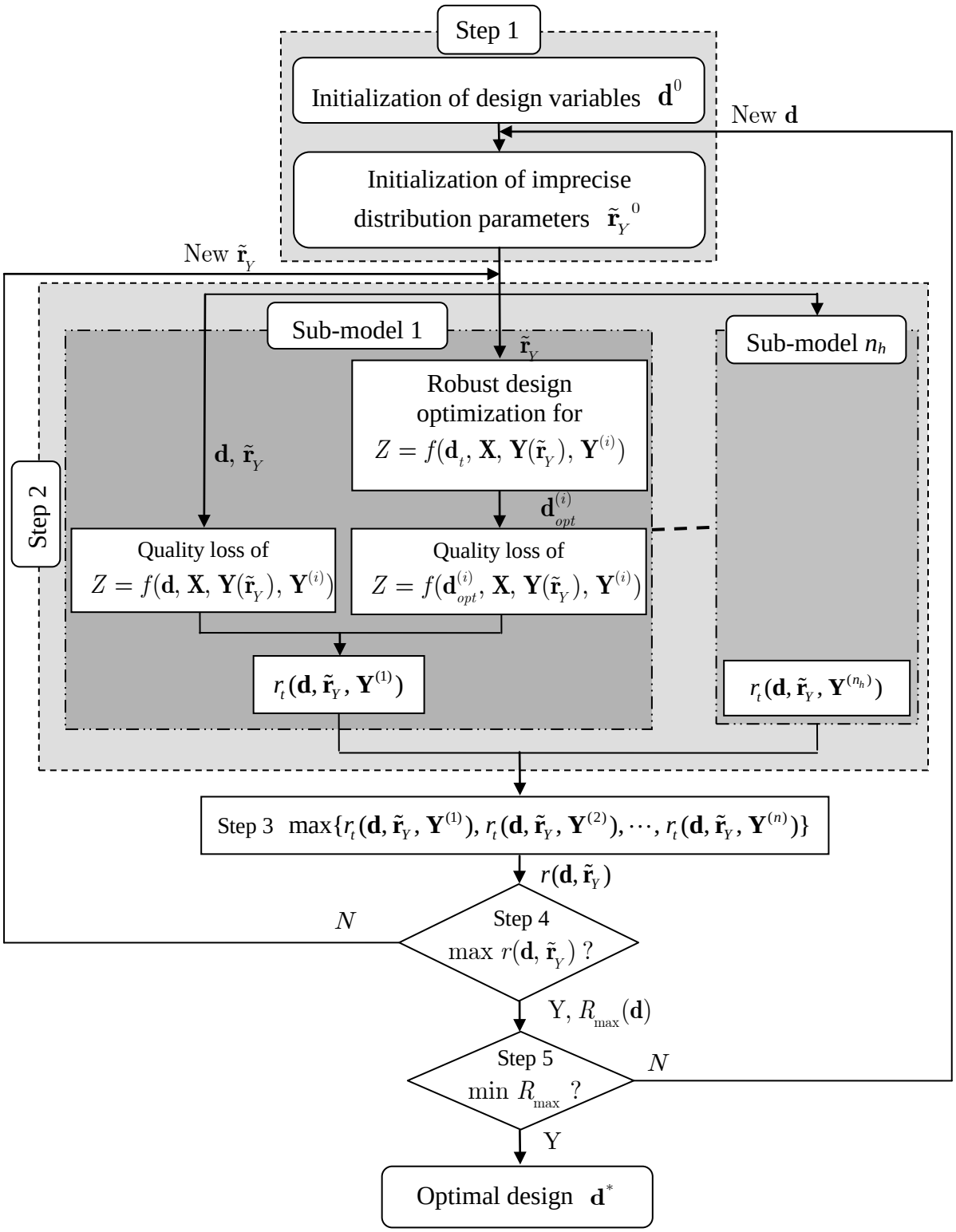

Fig. 8. Flowchart of the third robust design optimization model

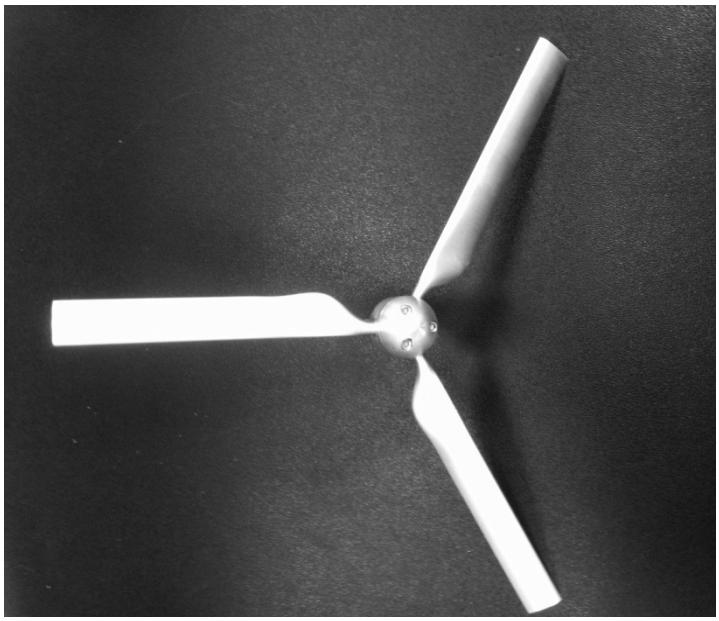

Fig. 9. Prototype of a Hydrokinetic turbine

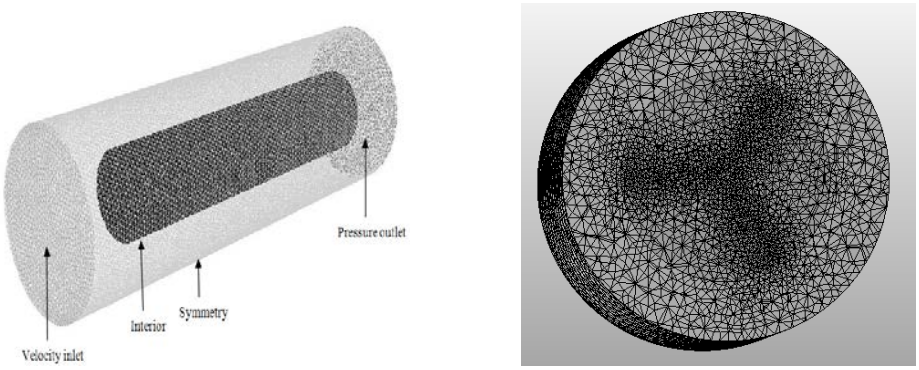

(a) (b)

Fig.10 (a) Boundary conditions for 3D CFD model (b) CFD mesh-Local refinement

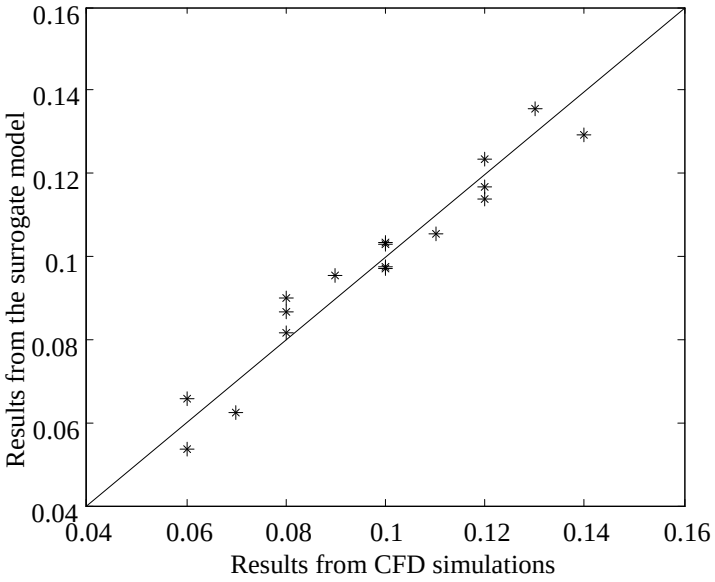

Fig. 11. Scatter diagram of the results obtained from CFD simulations and response surface model

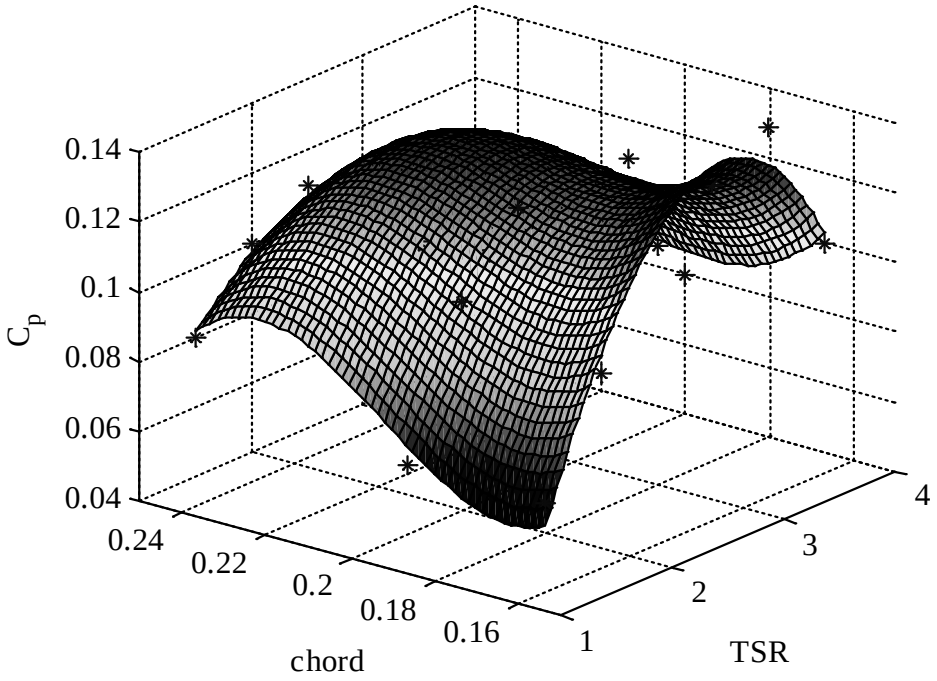

Fig. 12. Surrogate model of the power coefficient and data points from simulations

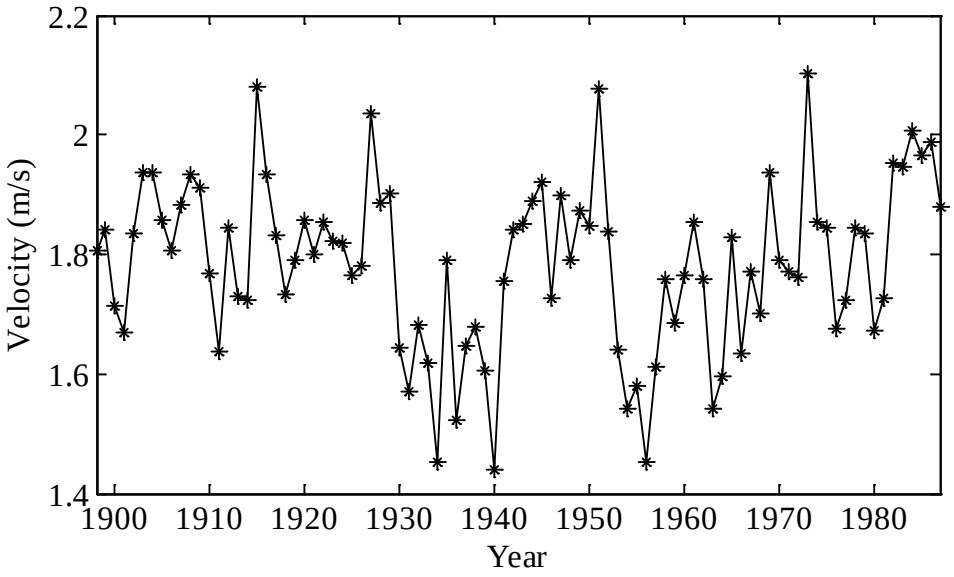

Fig. 13. Historical river velocity data of Missouri river at Hermann, Missouri station

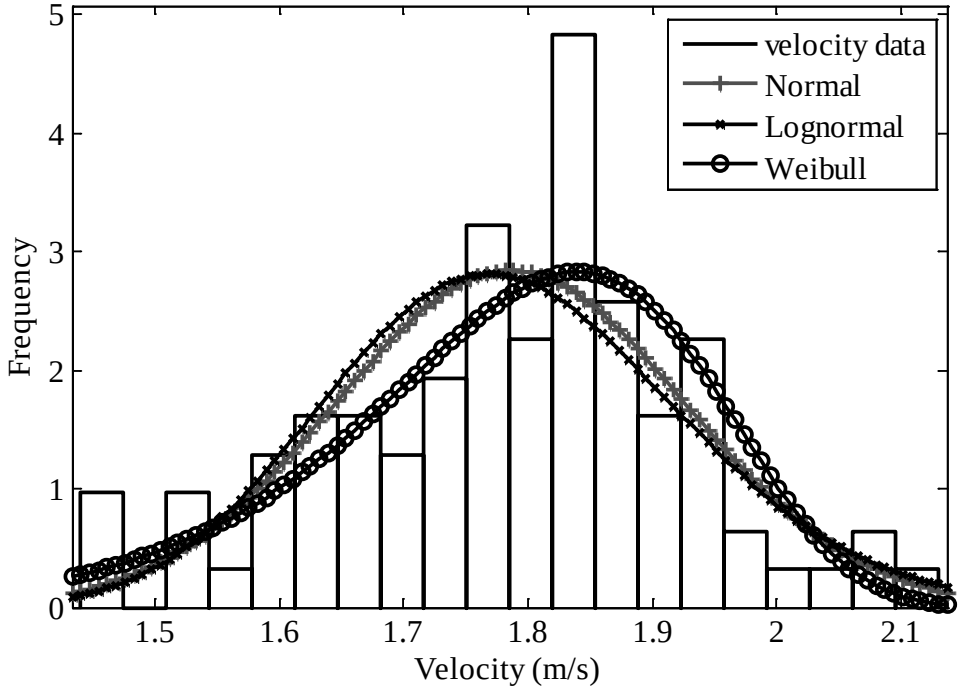

Fig. 14. Fitted distributions for the river velocity

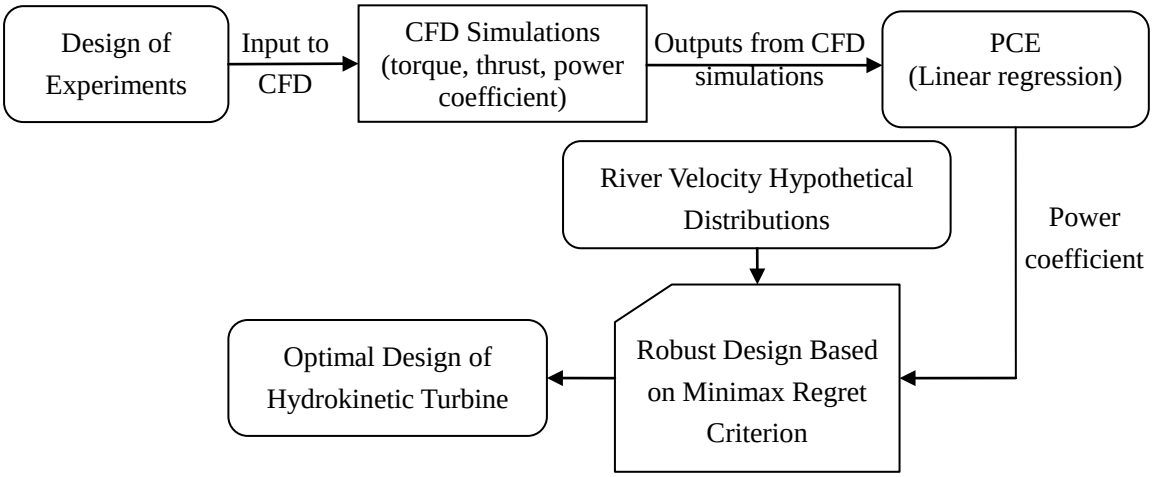

Fig. 15. Flowchart of robust design of hydrokinetic turbine

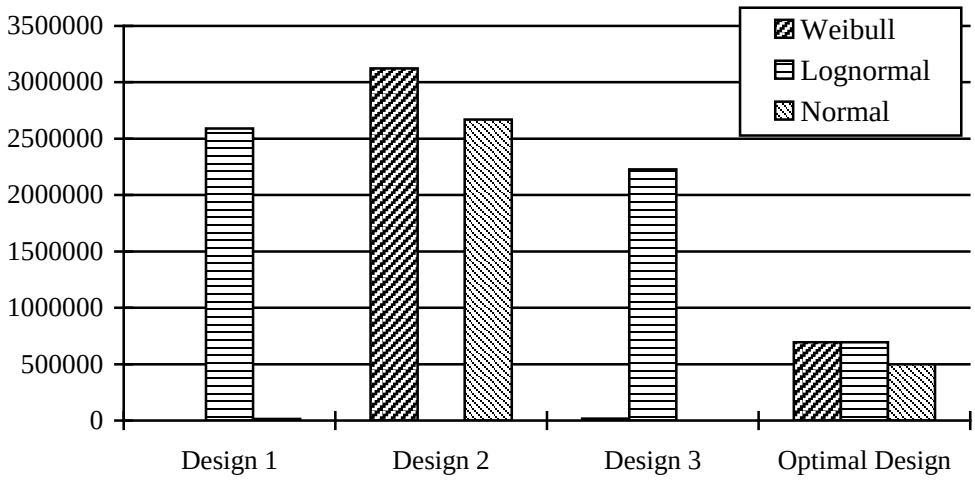

Fig. 16. Regret values of four different designs under different candidate distributions